Table II. *CA-AhR expression affects thymocyte population*[a]

	Line A (n = 4)		Line K (n = 5)		Line N (n = 5)	
	Wt	Tg	Wt	Tg	Wt	Tg
	(%)		(%)		(%)	
DN	4.7 ± 0.5[b]	6.4 ± 1.2	4.2 ± 1.1	52.6 ± 7.8	6.8 ± 2.8	27.9 ± 14.1
DP	82.2 ± 1.7	79.3 ± 1.4	87.2 ± 1.8	33.5 ± 7.6	83.2 ± 2.4	53.1 ± 15.9
CD4 SP	10.0 ± 1.5	9.5 ± 2.0	6.9 ± 0.7	8.7 ± 1.2	7.0 ± 0.8	10.2 ± 0.9
CD8 SP	3.1 ± 0.2	4.9 ± 0.4	1.8 ± 0.4	5.2 ± 0.5	3.1 ± 0.3	8.8 ± 1.2
CD4/CD8[c]	2.6 ± 1.1	2.0 ± 0.5	4.0 ± 0.7	1.8 ± 0.6**	2.3 ± 0.3	1.2 ± 0.1**

[a] Thymocytes from female heterozygous (CA-AhR$^{+/-}$) Tg mice and nontransgenic (CA-AhR$^{-/-}$) littermate mice (Wt) (8–10 wk old) were examined by flow cytometry. [b] The data was expressed as means ± S.D. The differences between CD4/CD8 ratio in Tg mice and Wt mice were evaluated with Wilcoxon rank sum test. **, $p < 0.01$. [c] Ratio of CD4 SP cells/CD8 SP cells.

whole thymus and the stroma (Fig. 6). CA-AhR was detected only in whole thymus, not in the stroma, in this system (Fig. 6). Thus, AhR activation in thymocytes alone was demonstrated to cause the cellular loss and population changes in the thymus.

CA-AhR suppresses the increase in spleen weight and splenocyte number caused by immunization

We previously reported finding that TCDD administration to mice immunized with OVA suppressed the immunization-induced increase in spleen weight and splenocyte number (27, 34). Consistent with these findings, the increase in spleen weight and splenocyte number observed in wild-type mice after immunization with OVA was suppressed in line A Tg mice (Fig. 7), although their spleen was unaffected when not immunized, as stated above (Fig. 5). Interestingly, increases of both CD4 T cells and B cells were significantly suppressed despite the specific expression of CA-AhR in T cells (Fig. 7). The number of CD8 T cells was also fewer in the Tg mice than in the wild-type mice, although the difference was not significant. Simultaneous suppression of the T and B cell increase was also observed in OVA-immunized and TCDD-exposed wild-type mice (27).

To estimate how much TCDD induces the corresponding level of AhR activation, CYP1A1 expression in the thymus and spleen of line A Tg mice and TCDD-exposed wild-type mice was compared. As shown in Fig. 8, the level of expression of CYP1A1 mRNA in the thymus of the Tg mice was slightly higher than its level of expression in wild-type mice exposed to a single dose of 20 μg/kg TCDD. CYP1A1 expression in the spleen of the Tg mice was less than in wild-type mice exposed to 20 μg/kg TCDD, which seems plausible because only T cells express CYP1A1 mRNA in the spleen of Tg mice, whereas both T and B cells express CYP1A1 mRNA in TCDD-exposed wild-type mice (43). These results show that the function of the activated AhR in line A heterozygous mice and AhR activated by 20 μg/kg TCDD are roughly comparable. In our previous study, 20 μg/kg TCDD suppressed the splenocyte number to 60% of the number in unexposed control mice 1 wk after immunization (27). The same dose of TCDD reduced the thymus weights to 40–60% (44). The fact that a similar extent of suppression was observed in the thymus and spleen of the Tg mice indicates that the major portion of the effect of TCDD in these organs is attributable to AhR activation in the T cells.

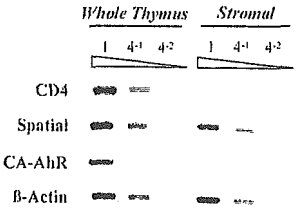

FIGURE 6. CA-AhR is expressed in the thymocytes, but not in the stromal cells, in the thymus. line A male CA-AhR$^{+/+}$ mice were mated with female C57BL/6J mice, and thymuses were collected from fetuses on gestational day 16.5. The thymuses were cultured for 4 days on a nitrocellulose filter floated on complete medium. To deplete them of thymocytes and obtain stromal cells, the lobes were cultured in the presence of 1.35 mM 2-deoxyguanosine. Fifteen or 16 lobes were pooled from each treatment group and were used to prepare RNA. cDNAs prepared from 20 ng of total RNA and serial dilutions (4^{-1}, 4^{-2}) were amplified by PCR

Discussion

To prove the role of activated AhR in T cells in TCDD-induced immune suppression, we generated Tg mice in which expression of CA-AhR cDNA is controlled by an improved version of hCD2 promoter and their T cells specifically express activated form of AhR. We obtained three lines bearing different copy numbers of the transgene, ranging from 2 to 10. All three lines showed expression of CA-AhR and an AhR-induced target gene in the thymus and spleen. In line A mice, which coexpress GFP in addition to CA-AhR under the control of the same CD2 promoter, the transgene was confirmed to be strongly expressed in the thymocytes, CD4, and CD8 T cells, but not in the thymus stromal cells or in the B cells. CD2 is principally expressed on T cells and NK cells in humans (45), but low expression has also been reported on subsets of other cell types, including B cell progenitors (46, 47). Consistent with the observation, faint expression of the transgene was detected on the CD3$^-$CD127$^+$ lymphocyte progenitor cells in our

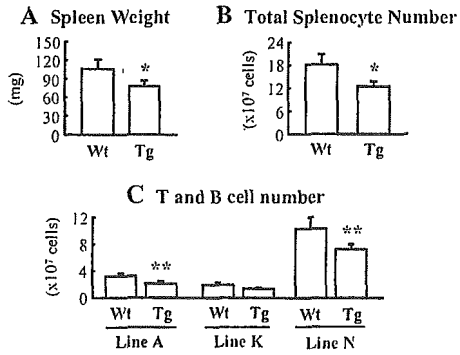

FIGURE 7. CA-AhR expression suppresses the increase in spleen weight and both CD4 T cell and B cell numbers after immunization. Line A female heterozygous Tg mice and littermate wild-type mice (8 wk old, n = 4) were immunized with OVA/alum, and their spleens were examined 7 days later. Mice were used after crossing into C57BL/6 mice for five generations. The differences between the Tg mice and wild-type mice were analyzed by Student's t test. The data are expressed as mean ± SD. *, $p < 0.05$; **, $p < 0.01$.

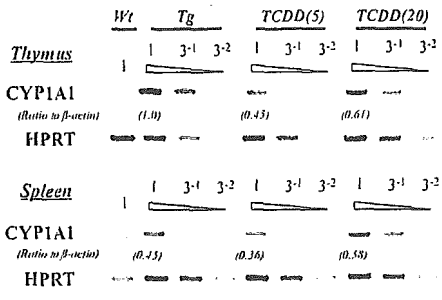

FIGURE 8. Comparison of CYP1A1 induction by CA-AhR in Tg mice and by TCDD exposure. Female C57BL/6 mice were given 5 or 20 μg/kg TCDD, and 3 days later total RNAs were prepared from thymocytes and splenocytes. CYP1A1 induction was compared with its induction in female line A heterozygous mice. cDNAs prepared from 20 ng of total RNA and serial dilutions (3^{-1}, 3^{-2}) were amplified by PCR using primers for CA-AhR or hypoxanthine phosphoribosyltransferase as a housekeeping gene. The expression of genes was quantified by densitometrically scanning gel images, and the values normalized to β-actin mRNA are indicated in parentheses. In both tissues, 30 PCR cycles were used for CYP1A1 and 20 for hypoxanthine phosphoribosyltransferase.

Tg mice. The transgene was also found to be expressed in the lung and, to a very minor extent, in the kidney in the Tg mice. Although the mechanism for the expression of CA-AhR in those tissues is unknown, presence of cells expressing CA-AhR in those tissues, such as T cells in the lung, may partly contribute to the transgene expression. Albeit the expression of the vector is found in other cell types, these CD2-based vectors, including the VA hCD2 vector, have been proved to be very useful to study specific functions of molecules in T cells. Likewise, the Tg mice we developed in the present study enable a new approach to explore the effect of AhR activation in T cells in the immune suppression. Lymphocyte progenitor cells have been reported to be affected by TCDD, and its effect was suggested to contribute to a loss of thymocytes (48, 49). Although the expression of CA-AhR in the lymphocyte progenitor cells was much fainter than that in the thymocytes and T cells (Figs. 2 and 3), the effects of low expression of CA-AhR may need to be considered.

All three lines of our Tg mice were characterized by thymus involution, including reduced thymocyte number and increased percentage of CD8 SP cells, the same as observed in TCDD-exposed mice. The fact that direct exposure of FTOC to TCDD reproduces the thymus involution induced by TCDD exposure in vivo (19, 24) shows that TCDD directly affects the thymus, in which the target cells are present. However, the results of previous studies have suggested that two types of cells in the thymus, thymocytes (18, 28) and stromal cells (24, 25), are the primary targets. The results of the present study in the Tg mice demonstrate that AhR activation in T-lineage cells alone can cause the thymus alterations, including loss of thymocytes and increase in percentage of CD8 SP thymocytes, without AhR activation in the stromal cells. Tomita et al. (50) recently produced T cell-specific ARNT-deficient mice in which the ARNT gene is disrupted under the control of T cell-specific $p56^{lck}$ proximal promoter, and showed that the thymus of the Tg mice is resistant to TCDD. Their results are consistent with our own showing that the AhR/ARNT heterodimer in the thymocytes, but not stromal cells, is essential for the occurrence of thymus involution.

Whereas thymus undergoes involution upon TCDD exposure, the splenocytes and splenic T cells of nonimmunized animals are unaffected by TCDD (18, 51). The same finding was observed in the spleen of our T cell-specific CA-AhR Tg mice, even though the CA-AhR was fully expressed in both the spleen T cells and the thymocytes. Although we examined the expression of CYP1A1 and adseverin as sensitive AhR-dependent target genes to estimate the extent of AhR activation, the genes responsible for the thymus involution remain to be identified. Previous studies have suggested suppression of thymocyte proliferation (24, 28) and induction of apoptosis (52) as the biological process involved in the thymus atrophy caused by TCDD. Our own recent study demonstrated that CA-AhR expression in Jurkat T cells inhibits cell growth by inducing both apoptosis and cell cycle arrest (29). Several genes in these CA-AhR-expressing Jurkat T cells that are related to apoptosis or cell cycle arrest, such as Fas, cyclin G_2, and growth arrest and DNA damage-inducible protein 34, were shown to be up-regulated in an XRE-mediated transcription-dependent manner (29), and these genes may be responsible for the loss of thymocytes.

In contrast with the nonimmunized mice in which splenocytes were less affected by AhR activation, as described above, the increase in splenocyte number after immunization was suppressed in the CA-AhR Tg mice, suggesting that the AhR/ARNT heterodimer inhibits cell growth in activated and proliferating T cells, but not in resting T cells. From this point of view, the effect of AhR activation in thymocytes may be also attributable to the effect on activated or proliferating cells: in thymus atrophy, the suppression of DN cell proliferation (28) and the loss of DP cells (52) are suggested to be responsible for cellular loss, DN thymocytes are vigorously proliferating cells, and DP cells receive an activation signal via their T cell receptors. Thus, activation state of the cell seems to affect the sensitivity of T-lineage cells to AhR activation.

The results of the present study also demonstrated that AhR activation in T cells alone suppresses the increase in both T and B cells in the spleen after OVA immunization. In terms of primary target cells of TCDD toxicity in immune reaction, Kerkvliet et al. (26) recently showed that AhR in both CD4 and CD8 T cells is necessary for full suppression of CTL response by TCDD in a mouse acute graft-vs-host model in which T cells, or CD4 or CD8 subsets, from $AhR^{+/+}$ and $AhR^{-/-}$ C57BL/6 mice were injected into C57BL/6 × DBA/2 F_1 host mice. Consistently, our results indicated that AhR activation in T cells is involved in changes in immune reaction. We previously reported that TCDD administration to OVA-immunized mice suppresses the growth of T and B cells and the production of Th2-type cytokines before suppression of Ab production (27, 34), which suggested that TCDD inhibits Ab production by suppressing T cell activation and the subsequent Th2-cell differentiation. The results of the present study strongly support the hypothesis that activation of the AhR directly inhibits cellular activation of the T cells and their subsequent proliferation and differentiation, leading to the suppression of T cell help on B cell proliferation. Alternatively, indirect effect of $CD4^+CD25^+$ regulatory T cells may be involved in the immune suppression. The regulatory T cells are positively selected in the thymus when their TCR receives a signal with intermediate strength (53). TCDD exposure to thymus is shown to affect thymocyte selection, possibly through up-regulation of Notch 1 (54) or activation of the ERK pathway (35) in the thymocytes, and these mechanism may alter the selection of $CD4^+CD25^+$ regulatory T cells. Further study of our Tg mice will clarify whether the suppression of T cell growth by AhR activation inhibits Th2-type cytokines and following Ab production by B cells, and it will also provide a clue for solving the mechanism of inhibition.

Andersson et al. (55) recently produced Tg mice expressing a CA-AhR mutant (30), which has a structure very similar to the one we used, under the control of an Ig H chain enhancer (Eμ), which promotes transgene expression in both B- and T-lineage cells (56). In addition to exhibiting thymus atrophy, their mice have a reduced life span and develop tumors in the glandular part of the stomach

(55). The Tg mice generated in our study, in contrast, are fertile and do not exhibit any overt phenotype differences except thymus atrophy, showing that AhR activation in T cells is not responsible for the stomach tumors.

Although T cells contain functional AhR and directly respond to TCDD (57), phenotypic changes caused by TCDD in T cells, such as changes in proliferation and differentiation, are difficult to detect *in vitro*, possibly because of optimized culture conditions that compensate for the effects of TCDD (6). The Tg mice expressing CA-AhR in T cells will be a useful model for investigating the role of activated AhR in the T cells. In particular, immunization of the Tg mice is expected to show suppression of various immune reactions, including Ab production and CTL activity, the same as observed in TCDD-exposed mice. Dioxins are persistent environmental contaminants and as such animals are continually exposed to them. TCDD maternally exposed is transferred to fetus and pups through the placenta or milk and activates their AhR (58, 59). Our Tg mice express CA-AhR mRNA in the fetal thymuses (data not shown) and the expression continues in the T-lineage cells after birth. Thus, these Tg mice will also be a useful model for clarifying the effect of persistent activation of AhR in T cells. Studies using our CA-AhR Tg mice should shed light on the role of the AhR in T cells in immune suppression by TCDD and also in physiological reactions.

Acknowledgments

We thank Y. Miyamoto, K. Ao, and M. Matsumoto for their excellent technical assistance, Drs. M. Kubo and R. Abe (Science University of Tokyo, Noda, Japan) for their useful discussions, and Drs. H. Toyoshiba and J. Yonemoto (National Institute for Environmental Studies, Tsukuba, Japan) for their valuable advice on statistics.

Disclosures

The authors have no financial conflict of interest.

References

1. Schmidt, J. V., and C. A. Bradfield. 1996. Ah receptor signaling pathways. *Annu. Rev. Cell Dev. Biol. 12:55.*
2. Mimura, J., and Y. Fujii-Kuriyama. 2003. Functional role of AhR in the expression of toxic effects by TCDD. *Biochim. Biophys. Acta 1619:263.*
3. Birnbaum, L. S., and J. Tuomisto. 2000. Non-carcinogenic effects of TCDD in animals. *Food Addit. Contam. 17:275.*
4. Dragan, Y. P., and D. Schrenk. 2000. Animal studies addressing the carcinogenicity of TCDD (or related compounds) with an emphasis on tumor promotion. *Food Addit. Contam. 17:289.*
5. Tohyama, C. 2002. Low-dose exposure to dioxin, its toxicities and health risk assessment. *Environ. Sci. 9:37.*
6. Kerkvliet, N. I. 2002. Recent advances in understanding the mechanisms of TCDD immunotoxicity. *Int. Immunopharmacol. 2:277.*
7. Lahvis, G. P., S. L. Lindell, R. S. Thomas, R. S. McCuskey, C. Murphy, E. Glover, M. Bentz, J. Southard, and C. A. Bradfield. 2000. Portosystemic shunting and persistent fetal vascular structures in aryl hydrocarbon receptor-deficient mice. *Proc. Natl. Acad. Sci. USA 97:10442.*
8. Fernandez-Salguero, P., T. Pineau, D. M. Hilbert, T. McPhail, S. S. T. Lee, S. Kimura, D. W. Nebert, S. Rudikoff, J. M. Ward, and F. J. Gonzalez. 1995. Immune system impairment and hepatic fibrosis in mice lacking the dioxin-binding Ah receptor. *Science 268:722.*
9. Robles, R., Y. Morita, K. K. Mann, G. I. Perez, S. Yang, T. Matikainen, D. H. Sherr, and J. L. Tilly. 2000. The aryl hydrocarbon receptor, a basic helix-loop-helix transcription factor of the PAS gene family, is required for normal ovarian germ cell dynamics in the mouse. *Endocrinology 141:450.*
10. Benedict, J. C., T.-M. Lin, I. K. Loeffler, R. E. Peterson, and J. A. Flaws. 2000. Physiological role of the aryl hydrocarbon receptor in mouse ovary development. *Toxicol. Sci. 56:382.*
11. Hushka, L. J., J. S. Williams, and W. F. Greenlee. 1998. Characterization of 2,3,7,8-tetrachlorodibenzofuran-dependent suppression and Ah receptor pathway gene expression in the developing mouse mammary gland. *Toxicol. Appl. Pharmacol. 152:200.*
12. Thurmond, T. S., J. E. Staples, A. E. Silverstone, and T. A. Gasiewicz. 2000. The aryl hydrocarbon receptor has a role in the *in vivo* maturation of murine bone marrow B lymphocytes and their response to 2,3,7,8-tetrachlorodibenzo-*p*-dioxin. *Toxicol. Appl. Pharmacol. 165:227.*
13. Petrulis, J. R., and G. H. Perdew. 2002. The role of chaperone proteins in the aryl hydrocarbon receptor core complex. *Chem. Biol. Interact. 141:25.*
14. Swanson, H. I. 2002. DNA binding and protein interactions of the AHR/ARNT heterodimer that facilitate gene activation. *Chem. Biol. Interact. 141:63.*
15. Marlowe, J. L., E. S. Knudsen, S. Schwemberger, and A. Puga. 2004. The aryl hydrocarbon receptor displaces P300 from E2F-dependent promoters and represses S-phase specific gene expression. *J. Biol. Chem. 279:29013.*
16. Tian, Y., A. B. Rabson, and M. A. Gallo. 2002. Ah receptor and NF-κB interactions: mechanisms and physiological implications. *Chem. Biol. Interact. 141:97.*
17. Ohtake, F., K. Takeyama, T. Matsumoto, H. Kitagawa, Y. Yamamoto, K. Nohara, C. Tohyama, A. Krust, J. Mimura, P. Chambon, et al. 2003. Modulation of oestrogen receptor signalling by association with the activated dioxin receptor. *Nature 423:545.*
18. Staples, J. E., F. G. Murante, N. C. Fiore, T. A. Gasiewicz, and A. E. Silverstone. 1998. Thymic alterations induced by 2,3,7,8-tetrachlorodibenzo-*p*-dioxin are strictly dependent on aryl hydrocarbon receptor activation in hemopoietic cells. *J. Immunol. 160:3844.*
19. Hundeiker, C., T. Pineau, G. Cassar, R. A. Betensky, E. Gleichmann, and C. Esser. 1999. Thymocyte development in Ah-receptor-deficient mice is refractory to TCDD-inducible changes. *Int. J. Immunopharmacol. 21:841.*
20. Vorderstrasse, B. A., L. B. Steppan, A. E. Silverstone, and N. I. Kerkvliet. 2001. Aryl hydrocarbon receptor-deficient mice generate normal immune responses to model antigens and are resistant to TCDD-induced immune suppression. *Toxicol. Appl. Pharmacol. 171:157.*
21. Lai, Z.-W., N. C. Fiore, T. A. Gasiewicz, and A. E. Silverstone. 1998. 2,3,7,8-Tetrachlorodibenzo-*p*-dioxin and diethylstilbestrol affect thymocytes at different stages of development in fetal thymus organ culture. *Toxicol. Appl. Pharmacol. 149:167.*
22. Nohara, K., H. Ushio, S. Tsukumo, T. Kobayashi, M. Kijima, C. Tohyama, and H. Fujimaki. 2000. Alterations of thymocyte development, thymic emigrants and peripheral T cell population in rats exposed to 2,3,7,8-tetrachlorodibenzo-*p*-dioxin. *Toxicology 145:227.*
23. Esser, C., and M. Welzel. 1993. Ontogenic development of murine fetal thymocytes is accelerated by 3,3′,4,4′-tetrachlorobiphenyl. *Int. J. Immunopharmacol. 15:841.*
24. Kremer, J., E. Gleichmann, and C. Esser. 1994. Thymic stroma exposed to receptor-binding xenobiotics fails to support proliferation of early thymocytes but induces differentiation. *J. Immunol. 153:2778.*
25. De Heer, C., E. J. De Waal, H.-J. Schuurman, J. G. Vos, and H. Van Loveren. 1994. The intrathymic target cell for the thymotoxic action of 2,3,7,8-tetrachlorodibenzo-*p*-dioxin. *Exp. Clin. Immunogenet. 11:86.*
26. Kerkvliet, N. I., D. M. Shepherd, and L. Baecher-Steppan. 2002. T lymphocytes are direct, aryl hydrocarbon receptor (AhR)-dependent targets of 2,3,7,8-tetrachlorodibenzo-*p*-dioxin (TCDD): AhR expression in both $CD4^+$ and $CD8^+$ T cells is necessary for full suppression of a cytotoxic T lymphocyte response by TCDD. *Toxicol. Appl. Pharmacol. 185:146.*
27. Ito, T., K. Inouye, H. Fujimaki, C. Tohyama, and K. Nohara. 2002. Mechanism of TCDD-induced suppression of antibody production: effect on T cell-derived cytokine production in the primary immune reaction of mice. *Toxicol. Sci. 70:46.*
28. Laiosa, M. D., A. Wyman, F. G. Murante, N. C. Fiore, J. E. Staples, T. A. Gasiewicz, and A. E. Silverstone. 2003. Cell proliferation arrest within intrathymic lymphocyte progenitor cells causes thymic atrophy mediated by the aryl hydrocarbon receptor. *J. Immunol. 171:4582.*
29. Ito, T., S. Tsukumo, N. Suzuki, H. Motohashi, M. Yamamoto, Y. Fujii-Kuriyama, J. Mimura, T.-M. Lin, R. E. Peterson, C. Tohyama, and K. Nohara. 2004. A constitutively active arylhydrocarbon receptor induces growth inhibition of Jurkat T cells through changes in the expression of genes related to apoptosis and cell cycle arrest. *J. Biol. Chem. 279:25204.*
30. McGuire, J., K. Okamoto, M. L. Whitelaw, H. Tanaka, and L. Poellinger. 2001. Definition of a dioxin receptor mutant that is a constitutive activator of transcription. *J. Biol. Chem. 276:41841.*
31. *Zhumabekov, T., P. Corbella, M. Tolaini, and D. Kioussis. 1995. Improved version of a human CD2 minigene based vector for T cell-specific expression in transgenic mice. J. Immunol. Methods 185:133.*
32. Motohashi, H., K. Igarashi, K. Onodera, S. Takahashi, H. Ohtani, M. Nakafuku, M. Nishizawa, J. D. Engel, and M. Yamamoto. 1996. Mesodermal- vs. neuronal-specific expression of MafK is elicited by different promoters. *Genes Cells 1:223.*
33. Nohara, K., H. Fujimaki, S. Tsukumo, K. Inouye, H. Sone, and C. Tohyama. 2002. Effects of 2,3,7,8-tetrachlorodibenzo-*p*-dioxin (TCDD) on T cell-derived cytokine production in ovalbumin (OVA)-immunized C57BL/6 mice. *Toxicology 172:49.*
34. Inouye, K., T. Ito, H. Fujimaki, Y. Takahashi, T. Takemori, X. Pan, C. Tohyama, and K. Nohara. 2003. Suppressive effects of 2,3,7,8-tetrachlorodibenzo-*p*-dioxin (TCDD) on the high-affinity antibody response in C57BL/6 mice. *Toxicol. Sci. 74:315.*
35. Tsukumo, S., M. Iwata, C. Tohyama, and K. Nohara. 2002. Skewed differentiation of thymocytes toward CD8 T cells by 2,3,7,8-tetrachlorodibenzo-*p*-dioxin requires activation of the extracellular signal-related kinase pathway. *Arch. Toxicol. 76:335.*
36. Jenkinson, E. J., L. L. Franchi, R. Kingston, and J. J. T. Owen. 1982. Effect of deoxyguanosine on lymphopoiesis in the developing thymus rudiment *in vitro*: application in the production of chimeric thymus rudiments. *Eur. J. Immunol. 12:583.*
37. Svensson, C., A. E. Silverstone, Z.-W. Lai, and K. Lundberg. 2002. Dioxin-induced adseverin expression in the mouse thymus is strictly regulated and dependent on the aryl hydrocarbon receptor. *Biochem. Biophys. Res. Commun. 291:1194.*

38. Li, W., S. Donat, O. Dohr, K. Unfried, and J. Abel. 1994. Ah receptor in different tissues of C57BL/6J and DBA/2J mice: use of competitive polymerase chain reaction to measure Ah-receptor mRNA expression. *Arch. Biochem. Biophys. 315:279.*
39. Song, J., M. Clagett-Dame, R. E. Peterson, M. E. Hahn, W. M. Westler, R. R. Sicinski, and H. F. DeLuca. 2002. A ligand for the aryl hydrocarbon receptor isolated from lung. *Proc. Natl. Acad. Sci. USA 99:14694.*
40. Kondo, M., I. L. Weissman, and K. Akashi. 1997. Identification of clonogenic common lymphoid progenitors in mouse bone marrow. *Cell 91:661.*
41. Wang, J.-F., Z.-Y. Liu, and J. E. Groopman. 1998. The α-chemokine receptor CXCR4 is expressed on the megakaryocytic lineage from progenitor to platelets and modulates migration and adhesion. *Blood 92:756.*
42. Flomerfelt, F. A., M. G. Kim, and R. H. Schwartz. 2000. Spatial, a gene expressed in thymic stromal cells, depends on three-dimensional thymus organization for its expression. *Genes Immun. 1:391.*
43. Nagai, H., T. Takei, C. Tohyama, M. Kubo, R. Abe, and K. Nohara. 2005. Search for the target genes involved in the suppression of antibody production by TCDD in C57BL/6 mice. *Int. Immunopharmacol. 5:331.*
44. Pan, X., K. Inouye, T. Ito, H. Nagai, Y. Takeuchi, Y. Miyabara, C. Tohyama, and K. Nohara. 2004. Evaluation of relative potencies of PCB126 and PCB169 for the immunotoxicities in ovalbumin (OVA)-immunized mice. *Toxicology 204:51.*
45. Moretta, A., E. Ciccone, G. Pantaleo, G. Tambussi, C. Bottino, G. Melioli, M. C. Mingari, and L. Moretta. 1989. Surface molecules involved in the activation and regulation of T or natural killer lymphocytes in humans. *Immunol. Rev. 111:145.*
46. Muraguchi, A., N. Kawamura, A. Hori, Y. Hirii, Y. Ichigi, M. Kimoto, and T. Kishimoto. 1992. Expression of the CD2 molecule on human B lymphoid progenitors. *Int. Immunol. 4:841.*
47. Crawford, K., D. Gabuzda, V. Pantazopoulos, J. Xu, C. Clement, E. Reinherz, and C. A. Alper. 1999. Circulating $CD2^+$ monocytes are dendritic cells. *J. Immunol. 163:5920.*
48. Silverstone, A. E., D. E. Frazier, Jr., and T. A. Gasiewicz. 1994. Alternate immune system targets for TCDD: lymphocyte stem cells and extrathymic T-cell development. *Exp. Clin. Immunogenet. 11:94.*
49. Murante, F. G., and T. A. Gasiewicz. 2000. Hemopoietic progenitor cells are sensitive targets of 2,3,7,8-tetrachlorodibenzo-*p*-dioxin in C57BL/6J mice. *Toxicol. Sci. 54:374.*
50. Tomita, S., H.-B. Jiang, T. Ueno, S. Takagi, K. Tohi, S. Maekawa, A. Miyatake, A. Furukawa, F. J. Gonzalez, J. Takeda, Y. Ichikawa, and Y. Takahama. 2003. T cell-specific disruption of arylhydrocarbon receptor nuclear translocator (*Arnt*) gene causes resistance to 2,3,7,8-tetrachlorodibenzo-*p*-dioxin-induced thymic involution. *J. Immunol. 171:4113.*
51. De Heer, C., A. P. J. Verlaan, A. H. Penninks, J. G. Vos, H.-J. Schuurman, and H. Van Loveren. 1994. Time course of 2,3,7,8-tetrachlorodibenzo-*p*-dioxin (TCDD)-induced thymic atrophy in the wistar rat. *Toxicol. Appl. Pharmacol. 128:97.*
52. Kamath, A. B., I. Camacho, P. S. Nagarkatti, and M. Nagarkatti. 1999. Role of Fas-Fas ligand interactions in 2,3,7,8-tetrachlorodibenzo-*p*-dioxin (TCDD)-induced immunotoxicity: increased resistance of thymocytes from Fas-deficient (*lpr*) and Fas ligand-defective (*gld*) mice to TCDD-induced toxicity. *Toxicol. Appl. Pharmacol. 160:141.*
53. Jonuleit, H., and E. Schmitt. 2003. The regulatory T cell family: distinct subsets and their interrelations. *J. Immunol. 171:6323.*
54. Kronenberg, S., Z.-W. Lai, and C. Esser. 2000. Generation of αβ T-cell $receptor^+$ $CD4^-CD8^+$ cells in major histocompatibility complex class I-deficient mice upon activation of the aryl hydrocarbon receptor by 2,3,7,8-tetrachlorodibenzo-*p*-dioxin. *Immunology 100:185.*
55. Andersson, P., J. McGuire, C. Rubio, K. Gradin, M. L. Whitelaw, S. Pettersson, A. Hanberg, and L. Poellinger. 2002. A constitutively active dioxin/aryl hydrocarbon receptor induces stomach tumors. *Proc. Natl. Acad. Sci. USA 99:9990.*
56. Bodrug, S. E., B. J. Warner, M. L. Bath, G. J. Lindeman, A. W. Harris, and J. M. Adams. 1994. Cyclin D1 transgene impedes lymphocyte maturation and collaborates in lymphomagenesis with the *myc* gene. *EMBO J. 13:2124.*
57. Doi, H., T. Baba, C. Tohyama, and K. Nohara. 2003. Functional activation of arylhydrocarbon receptor (AhR) in primary T cells by 2,3,7,8-tetrachlorodibenzo-*p*-dioxin. *Chemosphere 52:655.*
58. Abbott, B. D., J. E. Schmid, J. G. Brown, C. R. Wood, R. D. White, A. R. Buckalew, and G. A. Held. 1999. RT-PCR quantification of AHR, ARNT, GR, and CYP1A1 mRNA in craniofacial tissues of embryonic mice exposed to 2,3,7,8-tetrachlorodibenzo-*p*-dioxin and hydrocortisone. *Toxicol. Sci. 47:76.*
59. Nohara, K., H. Fujimaki, S. Tsukumo, H. Ushio, Y. Miyabara, M. Kijima, C. Tohyama, and J. Yonemoto. 2000. The effect of perinatal exposure to low doses of 2,3,7,8-tetrachlorodibenzo-*p*-dioxin on immune organs in rats. *Toxicology 154:123.*

A dioxin sensitive gene, mammalian *WAPL*, is implicated in spermatogenesis

Masahiko Kuroda[a,b,c,*], Kosuke Oikawa[a,b,c], Tetsuya Ohbayashi[a,b,c,1], Keiichi Yoshida[a,c], Kazuhiko Yamada[d], Junsei Mimura[e], Yoichi Matsuda[d], Yoshiaki Fujii-Kuriyama[e], Kiyoshi Mukai[a]

[a] *Department of Pathology, Tokyo Medical University, 6-1-1 Shinjuku, Shinjuku-ku, Tokyo 160-8402, Japan*
[b] *CREST Research Project, Japan Science and Technology Corporation, 4-1-6 Kawaguchi, Saitama 332-0012, Japan*
[c] *Shinanomachi Research Park, Keio University, 35 Shinanomachi, Shinjuku-ku, Tokyo 160-8582, Japan*
[d] *Chromosome Research Unit, Faculty of Science, Hokkaido University, North 10 West 8, Kita-ku, Sapporo 060-0810, Japan*
[e] *Center for Tsukuba Advanced Research Alliance, University of Tsukuba, 1-1-1 Tenno-dai, Tsukuba, Ibaraki 305- 8577, Japan*

Received 26 October 2004; accepted 13 November 2004

Available online 2 December 2004

Edited by Lukas Huber

Abstract 2,3,7,8-Tetrachlorodibenzo-*p*-dioxin (TCDD) is an endocrine disruptor that produces a variety of toxic e ects. We have isolated a mouse homolog of the *hWAPL* gene, termed *mouse WAPL* (*mWAPL*), as a target of TCDD by cDNA representational di erence analysis from mouse embryonic stem cells. A statistically significant increase in *mWAPL* expression was observed at 0.1 μM TCDD in AhR $^{-/-}$ mouse embryonic fibroblast cells. Interestingly, at 1 μM TCDD, *mWAPL* mRNA levels decreased in AhR$^{+/+}$ cells, but further increased in AhR $^{-/-}$ cells. *hWAPL* and mWAPL were highly expressed only in testes among normal tissue samples, and we observed mWAPL localization in the synaptonemal complex of testicular chromosomes. In addition, mouse testes decreased the expression of *mWAPL* mRNA after a single intraperitoneal injection of TCDD. Thus, mammalian *WAPL* such as *hWAPL* and *mWAPL* may be involved in spermatogenesis and be target genes mediating the reproductive toxicity induced by TCDD.

Keywords: WAPL; 2,3,7,8-Tetrachlorodibenzo-*p*-dioxin; Spermatogenesis; Synaptonemal complex

1. Introduction

In *Drosophila melanogaster*, the protein encoded by the *wings apart-like* (*wapl*) gene regulates heterochromatin structure [1]. The *wapl* product is required to hold the sister chromatids of meiotic heterochromatin together. In addition, wapl is implicated in both heterochromatin pairing during female meiosis and the modulation of position-e ect variegation (PEV). Moreover, a *P*-element screen of *Drosophila* identified wapl as a modifier of chromosome inheritance [2]. Recently, we have identified a novel human gene *hWAPL* that is a homolog of *wapl* [3]. *hWAPL* is overexpressed in invasive human cervical cancers and is often associated with cervical carcinogenesis. However, the essential function of hWAPL in normal cells is still unknown.

Dioxins, classified as endocrine disruptors, are ubiquitous in the environment. 2,3,7,8-tetrachlorodibenzo-*p*-dioxin (TCDD) is the most toxic dioxin and causes a variety of effects, including immunotoxicity, hepatotoxicity, teratogenicity, and tumor promotion [4,5]. Changes in gene expression induced by TCDD and related chemicals are initiated by the binding of the compounds to the aryl hydrocarbon receptor (AhR). AhR then dimerizes with the aryl hydrocarbon receptor nuclear translocator to form a complex that interacts with gene regulatory elements containing a xenobiotic response element (XRE) motif [6]. AhR mediates many of the TCDD-induced changes in gene expression. Many of the target genes responsible for the symptoms of toxicity, however, remain unidentified.

Previously, we performed a cDNA representational di erence analysis (RDA) of the cDNA derived from mouse ES cells treated or not with TCDD in order to isolate genes induced by TCDD. This procedure identified three genes, temporarily termed *Dioxin Inducible Factor 1*, *2*, and *3* (*DIF-1*, *DIF-2*, and *DIF-3*), that were induced in TCDD-treated ES cells. *DIF-1* is identical to the gene encoding histamine releasing factor (HRF) [7] and *DIF-3* is the gene encoding a novel protein with a C2H2 zinc-finger domain [8]. However, *DIF-2* has not yet been characterized.

In this study, we have identified the gene corresponding to *DIF-2* as a mouse homolog of *wapl* and *hWAPL*, termed *mouse WAPL* (*mWAPL*). We have also confirmed the e ects of TCDD on *mWAPL* expression and investigated the localization of mWAPL protein in normal adult mice to reveal the participation of mWAPL in TCDD-induced toxicity.

2. Materials and methods

2.1. cDNA cloning and sequencing

To isolate the complete mWAPL cDNA, we used total RNA from mouse testes. The full-length mWAPL cDNA was amplified by reverse transcription-PCR with primers designed from a computer search. We determined the nucleotide sequence of the cDNA with an Applied Biosystems 310 automated DNA sequencer.

*Corresponding author. Fax: +81 3 3352 6335.
E-mail address: kuroda@tokyo-med.ac.jp (M. Kuroda).

[1] Present address: Horizontal Medical Research Organization, Kyoto University Faculty of Medicine, Yoshida-Konoe-cho, Sakyo-ku, Kyoto, 606-8501, Japan.

Abbreviations: TCDD, 2,3,7,8-tetrachlorodibenzo-*p*-dioxin; AhR, aryl hydrocarbon receptor; MEF, mouse embryonic fibroblast

0014-5793/$22.00
doi:10.1016/j.febslet.2004.11.070

2.2. Cell cultures and chemicals

AhR / embryos were generated from intercrossed AhR$^{+/}$ mice [9]. Mouse embryonic fibroblasts (MEFs) of wild-type or mutant genotypes were harvested from day 14.5 mouse embryos. MEFs were grown as previously described [10]. 2,3,7,8-Tetrachlorodibenzo-*p*-dioxin (TCDD) (Cambridge Isotope Laboratories, Inc., Andover, MA) was prepared in dimethylsulfoxide (DMSO).

2.3. RNA isolation, quantitative real time PCR, and Northern blot analysis

RNA isolation was performed as described [10]. First strand cDNA synthesis was performed as described [11]. Real time PCR analysis was performed using the Smart Cycler System (Cepheid, Sunnyvale, CA) with SYBR Green I (Cambrex, Washington, DC). Real time PCR utilized *mWAPL* specific primers, 5 -ACCTGGTGGAGTATAGTGCCC-3 and 5 -TGGCAGAGACACCCAAGAAGC-3 ; mouse *β-actin* specific primers, 5 -AGCCTTCCTTCTTGGGTATGG-3 and 5 -CACTTGCGGTGCACGATGGAG-3 ; or *CYP1A1* specific primers, 5 -TTTGGTTTGGGCAAGCGA-3 and 5 -GTCTAAGCCTGAAGATGC-3 . Reaction mixtures were denatured at 95 C for 30 s, then subjected to 40 PCR cycles at either 95 C for 3 s, 68 C for 30 s, and 86 C for 6 s for *mWAPL*, or 95 C for 3 s, 68 C for 30 s, and 85 C for 6 s for mouse *β-actin* and *CYP1A1*. mRNA levels of *mWAPL* and *CYP1A1* were determined by normalization of their signals to *β-actin* signals. We performed the experiments to evaluate mRNA levels in triplicate. The data were analyzed using Student s *t* test, and *P*s < 0.01 were considered to indicate significant di erences.

For Northern blot analysis, the 567-bp *Dpn*II fragment of *mWAPL* cDNA and a PCR-amplified mouse *β-actin* cDNA fragment using the primers described above were used as probes and labeled with ^{32}P using the Rediprime II random prime labeling system (Amersham Biosciences, Piscataway, NJ). To examine *hWAPL* expression in various human tissues, we used Human MTN Blot I, II and III (Clontech, #7760-1, #7759-1 and #7767-1, respectively).

2.4. Immunoblot analysis and Immunohistochemistry

To generate polyclonal antibodies against hWAPL, we immunized rabbit against a 6 histidine-tagged hWAPL COOH terminus (amino acids 814–1037) fusion protein and obtained an anti-hWAPL polyclonal antibody (480-02). The anti-hWAPL polyclonal antibody was used at the dilution of 1:2000 for Immunoblot analysis and Immunohistochemistry. Immunoblot analyses were performed as previously described [7]. Protein samples from adult mouse tissues were prepared in RIPA bu er [7] and quantified using the BioRad protein assay (Nippon Bio-Rad Laboratories, Tokyo, Japan). Immunohistochemical analysis was performed on formalin-fixed para n-embedded sections using Ventana HX System Benchmark (Ventana Medical Systems INC., Tucson, AZ). As a control of specificity, the anti-hWAPL polyclonal antibody (480-02) was pre-incubated for 18 h at 4 C with a recombinant hWAPL protein and then applied to immunohistochemistry.

2.5. Immunocytology

The slides with surface-spread spermatocyte nuclei were prepared for immunocytological analysis as previously described [12]. Then, the anti-hWAPL polyclonal antibody (480-02) was diluted 1:400 and used as the primary antibody. After incubation with the primary antibody, the slide was reacted with goat anti-rabbit IgG conjugated to fluorescein isothiocyanate. DNA was visualized by counter-staining with 4 , 6-diamidine-2-phenylindole (DAPI).

2.6. Animals and treatment

Guidelines for the care and use of animals were approved by the animal research center at Tokyo Medical University. C57/BL6 male mice (13 weeks old) were purchased from Oriental Yeast Co., Ltd. (Tokyo, Japan). Each mouse received one intraperitoneal injection of 200 μl saline and 12.5 μl DMSO containing TCDD at a dose of 600 μg/kg of body mass. Control mice were injected with the same solution without TCDD. Testis samples were harvested 24 h after injection and subjected to real time PCR analysis.

3. Results and discussion

3.1. Molecular cloning of mouse WAPL

Using BLAST, we found that the nucleotide sequence of the DNA fragment corresponding to *Dioxin Inducible Factor-2* (*DIF-2*) is included in mKIAA0261, which is a mouse KIAA-homolog [13]. This suggested that *DIF-2* might be a homolog of the *hWAPL* gene because *hWAPL* corresponds to the KIAA0261 cDNA fragment [3]. Thus, we renamed the *DIF-2* gene *mouse WAPL* (*mWAPL*). Based on the mKIAA0261 sequence, we cloned and confirmed the nucleotide sequence of the full-length coding region of the cDNA for *mWAPL* (Database Accession No. AB167349). Multiple sequence alignment of the proteins encoded by *mWAPL*, *hWAPL*, and *wapl* demonstrated that the three proteins are similar not only in the WAPL conserved region [3], but throughout the entire protein (Fig. 1) (mWAPL is 92% identical and 96% similar to hWAPL, and 24% identical and 45% similar to wapl). Thus, the protein encoded by *mWAPL* may be involved in heterochromatin organization, PEV modification and chromosome inheritance like the wapl protein in *Drosophila*.

3.2. E ects of TCDD on MEFs

To confirm the e ects of TCDD on *mWAPL* expression, we examined *mWAPL* mRNA levels in AhR$^{+/+}$ and AhR / MEFs treated with 0, 0.01, 0.1, and 1 μM TCDD for 2 h by Northern blot analysis. Although *mWAPL* signals were on the whole extremely weak and barely visualized by strong enhancement, we found that *mWAPL* mRNA levels in AhR / MEFs showed the highest at 1 μM TCDD; in AhR$^{+/+}$ MEFs, on the other hand, *mWAPL* mRNA level at 0.1 μM TCDD was maximum (Fig. 2A). The two hybridization signals observed for *mWAPL* are similar to those observed in Northern blots for *hWAPL* and, as previously discussed [3], may reflect the di erence of the length of the untranslated regions of the *WAPL* mRNAs.

To evaluate the *mWAPL* mRNA levels more accurately, we performed quantitative real time PCR analysis and confirmed the expression pattern of *mWAPL* mRNA in AhR$^{+/+}$ and AhR / MEFs (Fig. 2B). We did not find significant di erences of cell cycle profile of these MEF cells by flow cytometric analysis (data not shown). Thus, although further investigation is required, the *mWAPL* gene may be inducible by TCDD independent of the AhR-mediated pathway but downregulated by a direct target molecule of TCDD in the AhR-dependent pathway.

3.3. Expression of mammalian WAPL in testes

Our previous study showed that *hWAPL* is expressed only in uterine cervical cancer among human tumor and normal control tissue samples examined [3]. Here, we examined mWAPL expression in normal mouse tissues by Western blot analysis and detected strong expression of mWAPL protein in the testes (Fig. 3A). Therefore, we also investigated *hWAPL* expression in various normal human tissues by Northern blot analysis, and confirmed that *hWAPL* mRNA was expressed abundantly in the testes, with weak expression in all other normal human tissues (Fig. 3B). Two hybridization signals for *hWAPL* mRNAs were visible in testes similar to MEFs (Fig. 2A) and previously reported results in cervical cancer tissues [3].

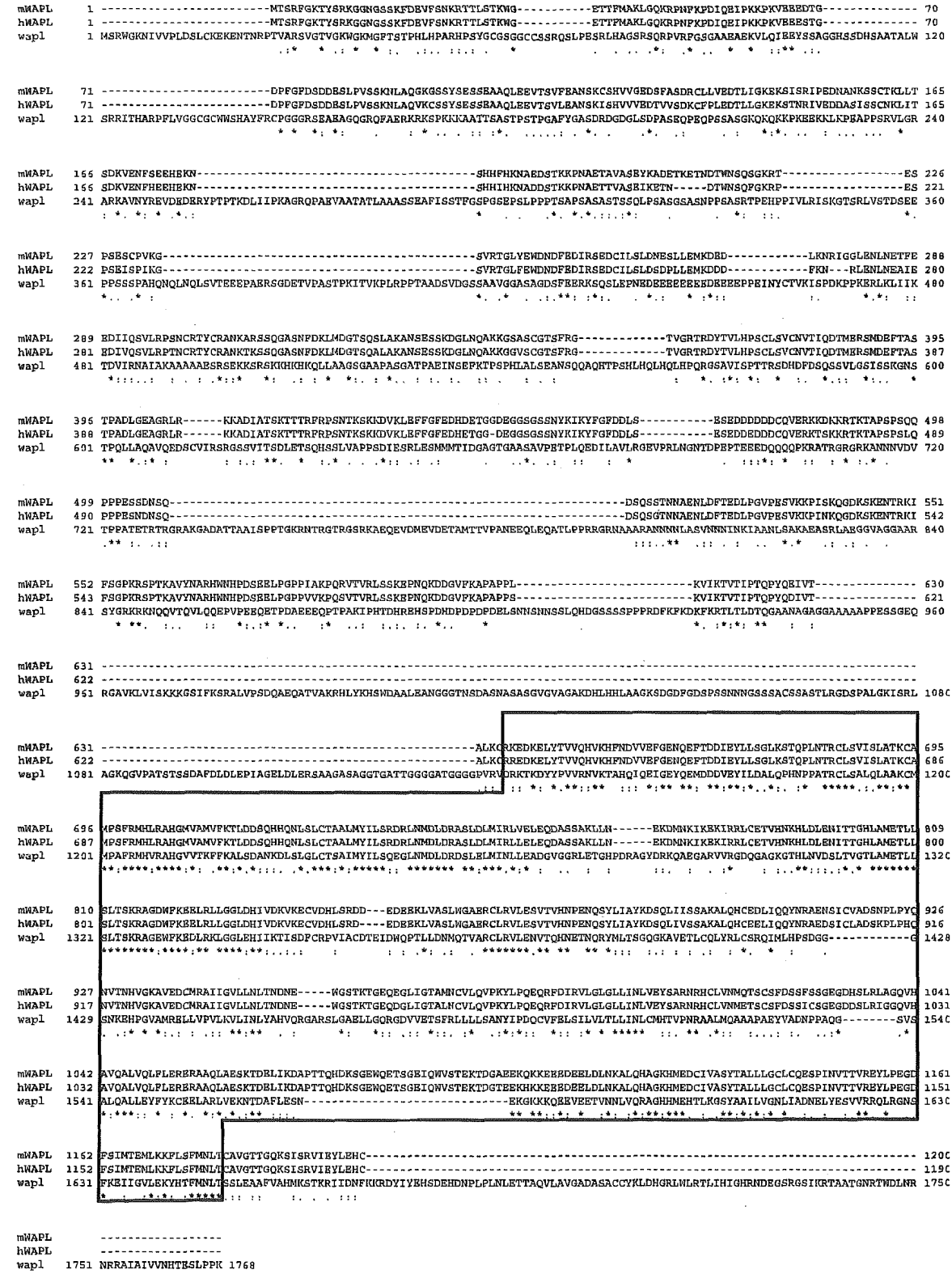

Fig. 1. Sequence alignment of WAPL homologs. The deduced amino acid sequences of mWAPL, hWAPL (Database Accession No. AB065003) and *Drosophila* wapl (Database Accession No. U40214) were aligned using CLUSTAL W multiple sequence alignment program. (*) indicates positions which have a single, fully conserved residue; (:) indicates that one of the following strong groups is fully conserved: (STA), (NEQK), (NHQK), (NDEQ), (QHRK), (MILV), (MILF), (HY) and (FYW); and ( ) indicates that one of the following weaker groups is fully conserved: (CSA), (ATV), (SAG), (STNK), (STPA), (SGND), (SNDEQK), (NDEQHK), (NEQHRK), (FVLIM), and (HFY). The boxed region indicates the WAPL-conserved region.

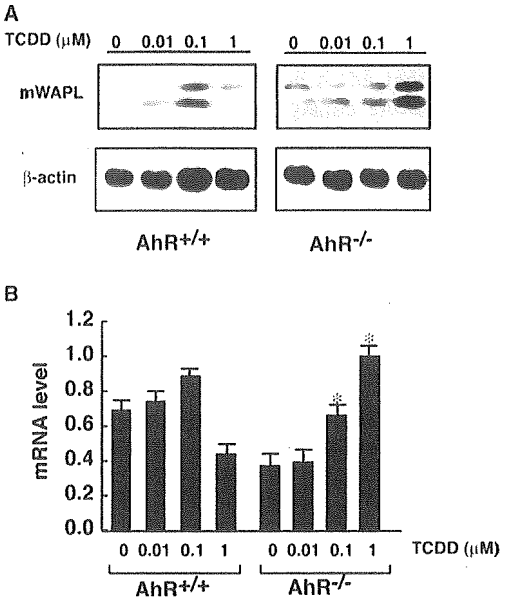

Fig. 2. E ects of TCDD on AhR$^{+/+}$ and AhR $^{/}$ MEFs. (A) Northern blot analysis of *mWAPL* in AhR$^{+/+}$ and AhR $^{/}$ MEFs treated with 0.1% DMSO and 0, 0.01, 0.1, or 1 μM TCDD for 2 h. The blots were hybridized with a probe for *mWAPL* (upper) and then reprobed with a *β-actin* probe as loading control (lower). (B) *mWAPL* mRNA levels in AhR$^{+/+}$ and AhR $^{/}$ MEFs treated with 0.1% DMSO and 0, 0.01, 0.1, or 1 μM TCDD for 2 h were determined with quantitative real time PCR analysis. The *mWAPL* mRNA levels were determined by normalization of *mWAPL* signals to *β-actin* signals, and the maximum mRNA expression level was arbitrarily set to 1 in the graphical presentation (*Y*-axis). The data were obtained from three independent experiments. Columns: means; bars: S.D. *, $P < 0.001$ versus the AhR $^{/}$ MEFs at 0 μM of TCDD.

We next examined the expression pattern of mWAPL in testes by immunohistochemical analysis using formalin-fixed mouse samples (Fig. 3C). The results showed that mWAPL was expressed abundantly in large pachytene spermatocytes, which are conspicuous for their size and loose organization of their chromatin, whereas it was undetectable in condensing forms of sperm (Fig. 3C, panel 2). We did not find any positive staining with the antibody after pre-absorption with a recombinant hWAPL protein (Fig. 3C, panel 3). These results suggested that mWAPL is expressed predominantly in early stages of spermatogenesis. similar results were observed in frozen sections (data not shown).

We have also characterized the subcellular localization of mWAPL in early spermatocytes by immunocytological staining. mWAPL immunoreactivity was detected at both zygotene (Fig. 3D) and pachytene stage (Fig. 3E). The antibody stained both unsynapsed and synapsed axial element components in early zygonema, and localized to the fully synapsed bivalents (synaptonemal complex) and the partially synapsed X and Y chromosomes (Fig. 3E, panel 3). From these results, hWAPL and mWAPL may be implicated in spermatogenesis. Although additional evidences are required, we suspect that mammalian WAPL may play a significant role in meiosis as does *Drosophila wapl* [1].

Furthermore, because of the localization of mWAPL in pachynema, we expect that mammalian WAPL functions in homologus recombination and DNA recombination. DNA double-strand breaks (DSB) constitute the most dangerous type of DNA damage induced by ionizing radiation.The gene

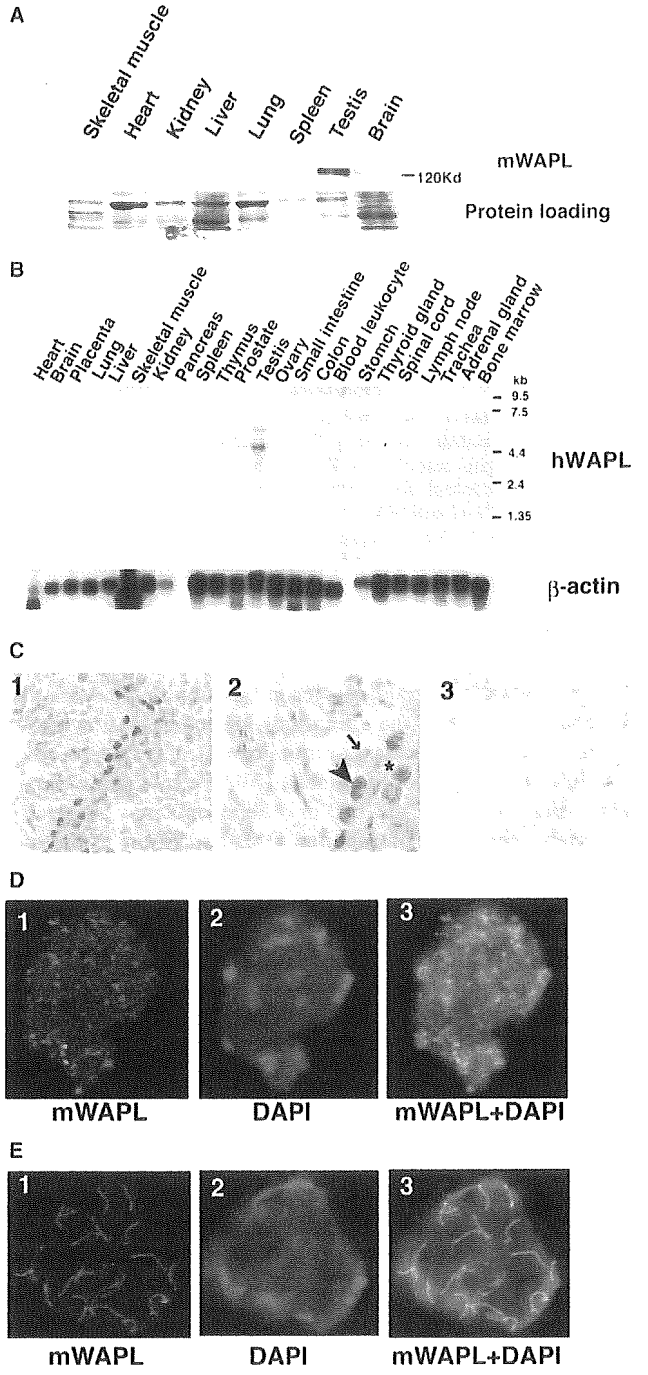

Fig. 3. Expression of mammalian WAPL in testes. (A) Western blot analysis of mWAPL in various normal mouse tissues. A Ponceau-stained nitrocellulose membrane is also shown as a control for protein loading (lower panel). (B) Northern blot analysis of *hWAPL* in various normal human tissues. *β-actin* signals are also shown as loading control. (C) mWAPL immunostaining in adult mouse testes. Formalin-fixed and para n-embedded 5 μm sections of mouse testes were treated with an anti-hWAPL antibody (panels 1 and 2), or the antibody after pre-absorption with a recombinant hWAPL protein as a negative control (panel 3), a horseradish peroxidase-conjugated secondary antibody, developed with diaminobenzidine, and counter-stained with hematoxylin. Specific cell types in the seminiferous epithelium are identified in panel 2: arrowhead, pachytene spermatocyte; arrow, round spermatid; asterisk, Sertoli cell. (D) Chromosomal spread of spermatocyte at early zygotene fixed and stained with anti-hWAPL antibody and DAPI (panel 1, mWAPL; panel 2, DAPI; panel 3, mWAPL + DAPI). (E) Chromosomal spread of spermatocyte at mid pachytene fixed and stained for mWAPL and DAPI (panel 1, mWAPL; panel 2, DAPI; panel 3, mWAPL + DAPI).

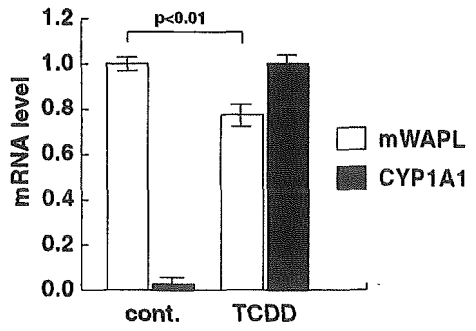

Fig. 4. Mouse testes exhibited a decreased level of mWAPL after TCDD treatment. *mWAPL* mRNA levels in testes of mice treated with or without TCDD (at a dose of 600 μg/kg of body mass) for 24 h were determined by quantitative real time PCR analysis. The data represent the means of eight samples. *CYP1A1* mRNA levels were also determined as a control for the e ects of TCDD on testes. The *mWAPL* and *CYP1A1* mRNA levels were determined by normalization of their signals to *β-actin* signals, respectively, and the maximum mRNA expression level was arbitrarily set to 1 in the graphical presentation (*Y*-axis). Bars: S.E.

that is implicated in homologous recombination might work at DSB repair [14,15] and the alterations in recombination promote carcinogenesis by causing genomic instability. Therefore, unscheduled expression of mammalian WAPL by human papilloma virus (HPV) [16], TCDD or other agents may cause an inaccurately repaired or unrepaired DSB and result in mutations or genomic rearrangements in surviving cells, which in turn leads to genomic instability and subsequently results in malignant cell transformation or defects in embryogenesis.

Recently, we have characterized another dioxin inducible gene named *Dioxin Inducible Factor 3* (*DIF-3*) that is highly expressed in testes [8]. Interestingly, DIF-3 is expressed most strongly in the large pachytene spermatocytes [8] similar to mWAPL. However, we have not found any evidence of functional association between mWAPL and DIF-3 until now.

3.4. Downregulation of mWAPL expression by TCDD in testes

These results prompted us to examine whether the expression of mWAPL was influenced by TCDD in testes. Twenty hours after the injection of TCDD into the abdominal cavities of C57/BL6 mice, we harvested the testes and analyzed *mWAPL* expression by quantitative real time PCR analysis. Because the *CYP1A1* gene is a well-known target of TCDD, we also calculated *CYP1A1* mRNA levels to confirm the effects of TCDD on testes. The mice exhibited a decrease in *mWAPL* expression and a marked increase in *CYP1A1* expression compared to control mice (Fig. 4). This result suggests that TCDD exposure a ects mWAPL expression levels in testes.

In recent years, several reports have focused on certain man-made toxins known as endocrine disrupting chemicals (EDCs) that persist in the environment. These chemicals are capable of altering the endocrine homeostasis of an animal, thereby causing serious reproductive and developmental defects as well as testicular oncogenesis [17–19]. Several studies have also provided evidence of a decline in semen quality and/or sperm counts over the same period [19]. Our previous study demonstrated that hWAPL overexpression induces carcinogenesis and tumor progression, and that hWAPL reduction by small interfering RNA (siRNA) induces cell death [3]. These observations suggest that unscheduled changes in hWAPL expression can cause severe damage to cells. Thus, although more experiments are needed to provide direct evidence linking mammalian *WAPL* with TCDD-induced reproductive toxicity, the present study suggests that mammalian *WAPL* may be a target gene mediating the reproductive toxicity of TCDD.

Acknowledgments: We thank E. Aoki, Y. Matsunaga, H. Sanai, S. Tsukamoto, and T. Hanashi for their expert technical assistance. This work was supported by a Grant-in-Aid for Scientific Research on Priority Area (C) (to M.K.) and a Grant-in-Aid for Encouragement of Young Scientists (to M.K.) from the Ministry of Education, Science, Sports and Culture, and Core Research for Evolutional Science and Technology (CREST) (to M.K.) from Japan Science and Technology Corporation.

References

[1] Verni, F., Gandhi, R., Goldberg, M.L. and Gatti, M. (2000) Genetic and molecular analysis of wings apart-like (wapl), a gene controlling heterochromatin organization in *Drosophila melanogaster*. Genetics 154, 1693–1710.
[2] Dobie, K.W., Kennedy, C.D., Velasco, V.M., McGrath, T.L., Weko, J., Patterson, R.W. and Karpen, G.H. (2001) Identification of chromosome inheritance modifiers in *Drosophila melanogaster*. Genetics 157, 1623–1637.
[3] Oikawa, K., Ohbayashi, T., Kiyono, T., Nishi, H., Isaka, K., Umezawa, A., Kuroda, M. and Mukai, K. (2004) Expression of a novel human gene, human wings apart-like (hWAPL), is associated with cervical carcinogenesis and tumor progression. Cancer Res. 64, 3545–3549.
[4] Chapman, D.E. and Schiller, C.M. (1985) Dose-related e ects of 2,3,7,8-tetrachlorodibenzo-*p*-dioxin (TCDD) in C57BL/6J and DBA/2J mice. Toxicol. Appl. Pharmacol. 78, 147–157.
[5] McGregor, D.B., Partensky, C., Wilbourn, J. and Rice, J.M. (1998) An IARC evaluation of polychlorinated dibenzo-*p*-dioxins and polychlorinated dibenzofurans as risk factors in human carcinogenesis. Environ. Health Perspect. 106 (Suppl. 2), 755–760.
[6] Sogawa, K. and Fujii-Kuriyama, Y. (1997) Ah receptor, a novel ligand-activated transcription factor. J. Biochem. (Tokyo) 122, 1075–1079.
[7] Oikawa, K., Ohbayashi, T., Mimura, J., Fujii-Kuriyama, Y., Teshima, S., Rokutan, K., Mukai, K. and Kuroda, M. (2002) Dioxin stimulates synthesis and secretion of IgE-dependent histamine-releasing factor. Biochem. Biophys. Res. Commun. 290, 984–987.
[8] Ohbayashi, T., et al. (2001) Dioxin induces a novel nuclear factor, DIF-3, that is implicated in spermatogenesis. FEBS Lett. 508, 341–344.
[9] Mimura, J., et al. (1997) Loss of teratogenic response to 2,3,7,8-tetrachlorodibenzo-*p*-dioxin (TCDD) in mice lacking the Ah (dioxin) receptor. Genes Cells 2, 645–654.
[10] Oikawa, K., et al. (2001) Dioxin suppresses the checkpoint protein, MAD2, by an aryl hydrocarbon receptor-independent pathway. Cancer Res. 61, 5707–5709.
[11] Kuroda, M., Ishida, T., Takanashi, M., Satoh, M., Machinami, R. and Watanabe, T. (1997) Oncogenic transformation and inhibition of adipocytic conversion of preadipocytes by TLS/FUS-CHOP type II chimeric protein. Am. J. Pathol. 151, 735–744.
[12] Matsuda, Y., Moens, P.B. and Chapman, V.M. (1992) Deficiency of X and Y chromosomal pairing at meiotic prophase in spermatocytes of sterile interspecific hybrids between laboratory mice (*Mus domesticus*) and *Mus spretus*. Chromosoma 101, 483–492.
[13] Okazaki, N., et al. (2003) Prediction of the coding sequences of mouse homologues of KIAA gene: III. the complete nucleotide sequences of 500 mouse KIAA-homologous cDNAs identified

by screening of terminal sequences of cDNA clones randomly sampled from size-fractionated libraries. DNA Res. 10, 167–180.
[14] Kuroda, M., et al. (2000) Male sterility and enhanced radiation sensitivity in TLS(/) mice. EMBO J. 19, 453–462.
[15] Willers, H., Dahm-Daphi, J. and Powell, S.N. (2004) Repair of radiation damage to DNA. Br. J. Cancer 90, 1279–1301.
[16] Kuroda, M., Kiyono, T., Oikawa, K., Yoshida, K. and Mukai, K. Br. J Cancer (in press).
[17] Birnbaum, L.S. (1995) Developmental e ects of dioxins and related endocrine disrupting chemicals. Toxicol. Lett. 82–83, 743–750.
[18] Brouwer, A., et al. (1995) Functional aspects of developmental toxicity of polyhalogenated aromatic hydrocarbons in experimental animals and human infant. Eur. J. Pharmacol. 293, 1–40.
[19] Sharpe, R.M. and Skakkebaek, N.E. (1993) Are oestrogens involved in falling sperm counts and disorders of the male reproductive tract?. Lancet 341, 1392–1395.

Available online at www.sciencedirect.com
SCIENCE DIRECT®
Biochemical and Biophysical Research Communications 337 (2005) 708–712
BBRC
www.elsevier.com/locate/ybbrc

CYP1A1-mediated mechanism for atherosclerosis induced by polycyclic aromatic hydrocarbons

Shunsuke Iwano, Fumie Asanuma, Manabu Nukaya, Tetsuya Saito, Tetsuya Kamataki *

Laboratory of Drug Metabolism, Graduate School of Pharmaceutical Sciences, Hokkaido University, Sapporo, Hokkaido, Japan

Received 7 September 2005
Available online 26 September 2005

Abstract

Polycyclic aromatic hydrocarbons (PAHs) have been known to induce atherosclerosis. It has been reported that the metabolic activation of PAHs by cytochrome P450 (CYP) is an important step for PAH-induced atherosclerosis. We recently reported that PAHs down-regulated the liver X receptor (LXR) α-regulated genes via aryl hydrocarbon receptor (AHR) as one of the causes responsible for atherosclerosis induced by PAHs. Thus, the aim of this study was to clarify the role of CYP1A1 in the suppression of LXR-mediated signal transductions by 3-methlychoranthrene (MC), one of the PAHs. We found that LXR-mediated transactivation was inhibited by the PAH, but not by halogenated aromatic hydrocarbon, which is scarcely metabolized by CYP1A1. The repression of LXR-mediated signal transductions by MC was restored by co-treatment of HepG2 cells with a CYP1A1 inhibitor, α-naphthoflavone, and by the transfection of short interference RNA for CYP1A1. Based on these lines of evidence, we propose that the metabolic activation of PAHs by CYP1A1, but not the activation of AHR by PAHs, is a direct mechanism for atherosclerosis via the suppression of LXR-mediated signal transductions.

Keywords: MC; Atherosclerosis; Metabolic activation; AHR; siRNA; Quantitative RT-PCR; Luciferase assay

Polycyclic aromatic hydrocarbons (PAHs)[1] are distributed widely and persistently in our environments. PAHs are generated through the combustion of fossil fuels, wood, and other organic materials [1]. Thus, the significant amounts of PAHs are found in automobile exhaust, cigarette smoke, charcoal-broiled foods, and the by-products of industrial waste [2–4]. A variety of toxicities, including carcinogenicity and atherogenesis, are caused by PAHs [5,6]. PAHs are generally known to produce the toxic effects through the activation of AHR [7–9]. However, detailed mechanisms responsible for the toxicities have remained unknown. AHR is a ligand-activated transcription factor that controls genes, including *CYP1A1*, *CYP1A2*, and *CYP1B1* [10].

CYP1A1 is an enzyme known to bioactivate carcinogenic compounds such as B[*a*]P, one of the typical PAHs [11]. The expression of CYP1A1 is induced by PAHs including B[*a*]P and MC via AHR [10,12]. Several reports have suggested that the metabolic activation of PAHs by CYPs, including CYP1A1, is a necessary step for PAH-induced atherosclerosis [5,6].

We recently demonstrated that MC inhibited LXR-mediated signal transductions through AHR, which are known to maintain the cholesterol homeostasis [13]. In the present study, we further investigated the role of CYP1A1 in the suppression of LXR-mediated signals by MC, since MC induces CYP1A1, as a more direct mechanism for

* Corresponding author. Fax: +81 11 706 4978.
E-mail address: SNC78123@nifty.com (T. Kamataki).

[1] *Abbreviations:* AH, aryl hydrocarbon; AHR, aryl hydrocarbon receptor; ANF, α-naphthoflavone; B[*a*]P, benzo[*a*]pyrene; CYP, cytochrome P450; DMEM, Dulbecco s modified Eagle s medium; FBS, fetal bovine serum; HAH, halogenated aromatic hydrocarbon; LXR, liver X receptor; LXRE, LXR response element; MC, 3-methylcholanthrene; PAH, polycyclic aromatic hydrocarbon; PCB, 3,4,3′,4′-tetrachlorobiphenyl; Res, resveratrol; RT-PCR, reverse transcriptase-polymerase chain reaction; siRNA, short interference RNA; T1317, TO-901317; TCDD, 2,3,7,8-tetrachlorodibenzo-*p*-dioxin; TK, thymidine kinase.

0006-291X/$ - see front matter
doi:10.1016/j.bbrc.2005.09.109

atherogenesis. In this paper, we show evidence indicating that CYP1A1 is a necessary factor for the MC-induced down-regulation of the LXR-target genes, suggesting that the metabolic activation of PAHs by CYP1A1 is a process critical for the repression of LXR-originated signal transductions by PAHs.

Materials and methods

Cell culture. Human hepatoma-derived HepG2 cells were purchased from RIKEN (Tsukuba, Japan). The HepG2 cells were maintained in DMEM (Nissui Pharmacy, Tokyo, Japan) supplemented with 10% FBS (BioWhittaker, Walkersville, MD), non-essential amino acids (ICN, Aurora, OH), and 1 mM sodium pyruvate (Gibco-BRL, Rockville, MD) in 5% CO_2 at 37 C.

Plasmids. Constructions of p(LXRE)$_2$-TK-Luc and pU6-siAHR were described previously [13]. Full-length human CYP1A1 cDNA was obtained by PCR with a sense primer, hCYP1A1-*Kpn*I-S (5′-CGGGGTACCGCC ATGCTTTTC-3′), and an antisense primer, hCYP1A1-*Bam*HI-AS (5′-CG GGATCCCTAAGAGCGCAGC-3′). The resultant fragment was digested with *Kpn*I and *Bam*HI, and inserted into the *Kpn*I and *Bam*HI sites of the pcDNA 3.1 mammalian expression vector (pcDNA-hCYP1A1) (Invitrogen, Carlsbad, CA). The pU6-siCYP1A1 as an siRNA expression plasmid for silencing the *CYP1A1* gene was constructed by using the p *Silencer* 1.0-U6 siRNA Expression Vector (Ambion, Austin, TX). To construct a hairpin siRNA expression cassette, two complementary oligonucleotides were synthesized, annealed, and ligated into the blunted *Apa*I site of the p*Silencer*. The sequences of the oligonucleotides were 5′-GGACGTGCTGCAG ATCCGAAttcaagagaTTCGGATCTGCACGTCCCCTTTTT-3′ and its complement, 5′-AAAAAGGGACGTGCTGCAGATCCGAAtctcttgaaT TCGGATCTGCAGCACGTCC-3′. This sequence cassette contained the oligonucleotides encoding 23-mer hairpin sequences specific for the human CYP1A1 mRNA at the 334-356 position, a ttcaagaga loop sequence separating the two complementary domains and a TTTTT terminator at the 3′-end [14–18].

Transient transfection and luciferase assay. One day before transfection, cells were plated at a density of 1 10^5 cells/well in a 12-well plate. Cells were transfected with 350 ng p(LXRE)$_2$-TK-Luc, 100 ng pcDNA-hLXRα, and 50 ng pRL-TK vector (as an internal control for transfection) by using Fugene6 (Roche Diagnostics, Indianapolis, IN). The medium was changed to fresh DMEM containing 1 μM T1317, a LXR ligand (Sigma–Aldrich, St. Louis, MO), AHR ligands including MC (5 μM) (Sigma-Aldrich), B[*a*]P (5 μM) (Sigma–Aldrich), TCDD (10 nM) (AccuStandard, New Heven, CT) or PCB (10 μM) (AccuStandard), Res (10 μM), an AHR antagonist, (Sigma–Aldrich), and ANF (1 μM), a CYP1A1 inhibitor, (Sigma–Aldrich). Cells were harvested after incubation for 36 h. Luciferase activity was measured according to the method provided by the manufacturer. When siRNA expression vector was applied, cells were transfected with 300 ng pU6-siAHR, pU6-siCYP1A1 or pU6-control, 100 ng pcDNA-hLXRα and pcDNA-hCYP1A1, 100 ng p(LXRE)$_2$-TK-Luc, and 50 ng pRL-TK vector. Twenty-four hours later, the medium was changed to DMEM containing MC (5 μM) and T1317 (1 μM). After incubation for 36 h, luciferase activity was measured.

Real-time RT-PCR analysis. HepG2 cells were transfected with 500 ng pU6-siAHR, pU6-siCYP1A1 or pU6-control. Twenty-four h after the transfection, the medium was changed to DMEM containing 10 μM MC and 1 μM T1317. After incubation for 24 h, total RNA from these cells was prepared using a GenElute Mammalian Total RNA Miniprep Kit (Sigma–Aldrich). Reverse transcription reaction was performed by using a First Strand cDNA Synthesis Kit for RT-PCR (AMV) (Roche Diagnostics). Quantitative real-time PCR was performed as described previously [13].

Results and discussion

To examine whether or not the metabolic activation of PAHs by CYPs was a necessary step for the PAH-induced suppression of LXR-signal transductions, the e ects of PAHs and HAHs on LXR-mediated transcriptional activity were investigated by a luciferase reporter assay (Fig. 1). When HepG2 cells were treated with MC and B[*a*]P, which are typical PAHs and readily metabolized by CYP1A1, the luciferase activity seen with p(LXRE)$_2$-TK-Luc decreased to a level of approximately 40–50% of control (Fig. 1). However, the luciferase activity was not a ected by the treatment with TCDD and PCB, which are typical HAHs and scarcely metabolized by CYP1A1 (Fig. 1). These results probably support the idea that the metabolic activation of PAHs by CYPs including CYP1A1 is a key step

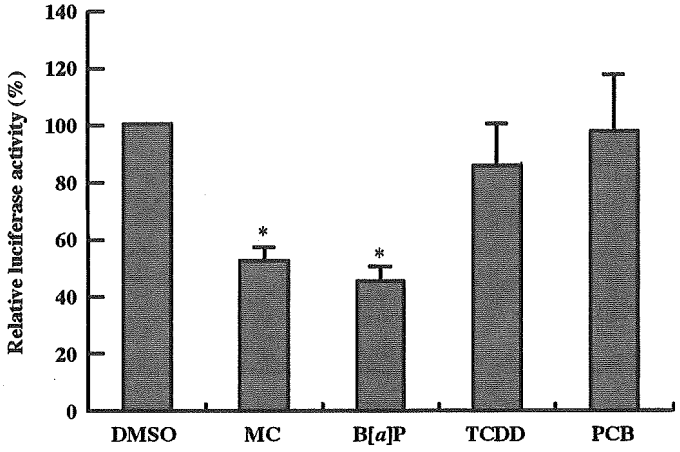

Fig. 1. Inhibition of LXR-mediated transcriptional activity by PAHs, but not by HAHs. HepG2 cells were transfected with p(LXRE)$_2$-TK-Luc and pcDNA-hLXRα in the presence of 1 μM T1317 and 5 μM MC, 5 μM B[*a*]P, 10 nM TCDD or 10 μM PCB. Luciferase activity was measured after incubation for 36 h. The values represent the average ±SD from three independent experiments. *Statistically di erent ($p < 0.05$) relative to the cells treated with T1317 alone.

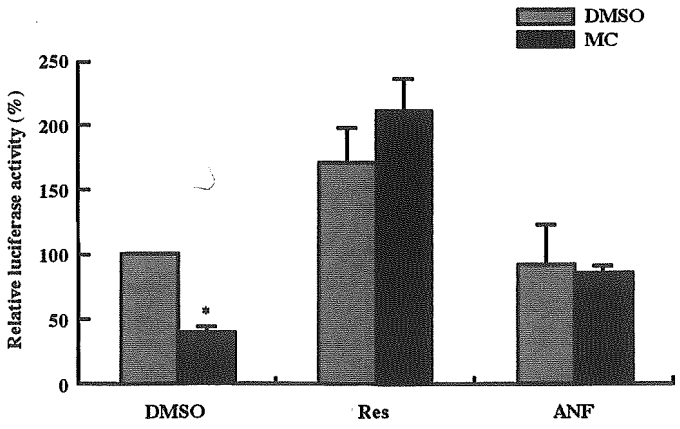

Fig. 2. E ects of Res, an AHR antagonist, and ANF, a CYP1A1 inhibitor, on the MC-induced suppression of LXR transactivation. A luciferase reporter plasmid, p(LXRE)$_2$-TK-Luc, was co-transfected into HepG2 cells with pcDNA-hLXRα. HepG2 cells were treated with Res (10 μM) or ANF (1 μM) together with or without MC (5 μM). The luciferase activity was measured after incubation for 36 h. Values in the figure represent the average ±SD from three independent experiments. *Statistically di erent ($p < 0.05$) relative to the cells treated with T1317 alone.

for the suppression of LXR-mediated signal transductions by PAHs.

To further support the idea that CYP1A1 was responsible for the repression of LXR-mediated signal transductions by PAHs, the e ects of the inhibitor of CYP1A1 on the LXR-mediated transcriptional activity were investigated (Fig. 2). When HepG2 cells were treated with Res, an AHR antagonist [19,20], the MC-induced suppression of luciferase activity with the p(LXRE)$_2$-TK-Luc was restored (Fig. 2). This result was consistent with our previous finding that LXR-mediated signal transduction was suppressed by MC via an AHR-mediated mechanism [13]. Treatment of HepG2 cells with ANF, a CYP1A1 inhibitor, restored the inhibition by MC of LXR transactivation (Fig. 2).

To investigate if CYP1A1 played a direct role in the MC-induced suppression of LXR-mediated signal transductions, we examined the e ects of CYP1A1 siRNA on the inhibition by MC of LXR transactivation (Fig. 3). When HepG2 cells were transfected with the pU6-siCYP1A1 and pU6-siAHR, the expression of mRNA for CYP1A1 decreased to a level of approximately 40% of control (Fig. 3A), indicating that both siCYP1A1 and siAHR were able to impair the metabolic activation of MC by CYP1A1. When the pU6-siAHR was transfected into HepG2 cells, the inhibition of LXR transactivation by MC was also restored (Fig. 3B). When the pU6-siCYP1A1 was transfected into HepG2 cells, the MC-induced repression of LXR-mediated transcriptional

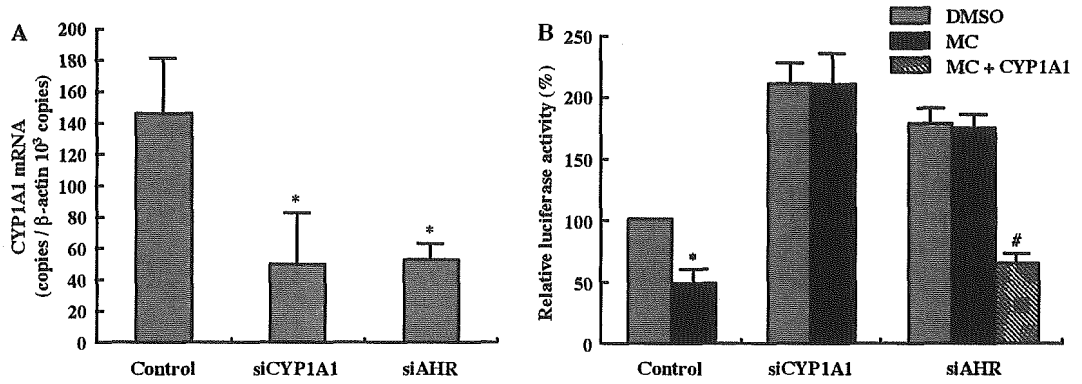

Fig. 3. E ects of siRNA for CYP1A1 on the MC-induced down-regulation of LXRα transactivation. (A) The expression of mRNA for CYP1A1 was quantified by real time RT-PCR. HepG2 cells were transfected with pU6-siAHR, pU6-siCYP1A1 or pU6-control, and then incubated with 5 μM MC. After incubation for 24 h, total RNA was prepared from these cells, and subjected to a real-time RT-PCR. (B) HepG2 cells were transfected with pcDNA-hLXRα, p(LXRE)$_2$-TK-Luc, and pU6-siCYP1A1 or pU6-siAHR. After incubation for 24 h, the cells were treated with T1317 in the presence or absence of MC. The luciferase activity was determined after incubation for 36 h. Values in the figure represent the average ±SD from three independent experiments. *Statistically di erent ($p < 0.05$) relative to the cells transfected with a control vector in the presence of T1317 alone. #Statistically di erent ($p < 0.05$) relative to the cells transfected with pU6-siAHR in the presence of T1317 alone.

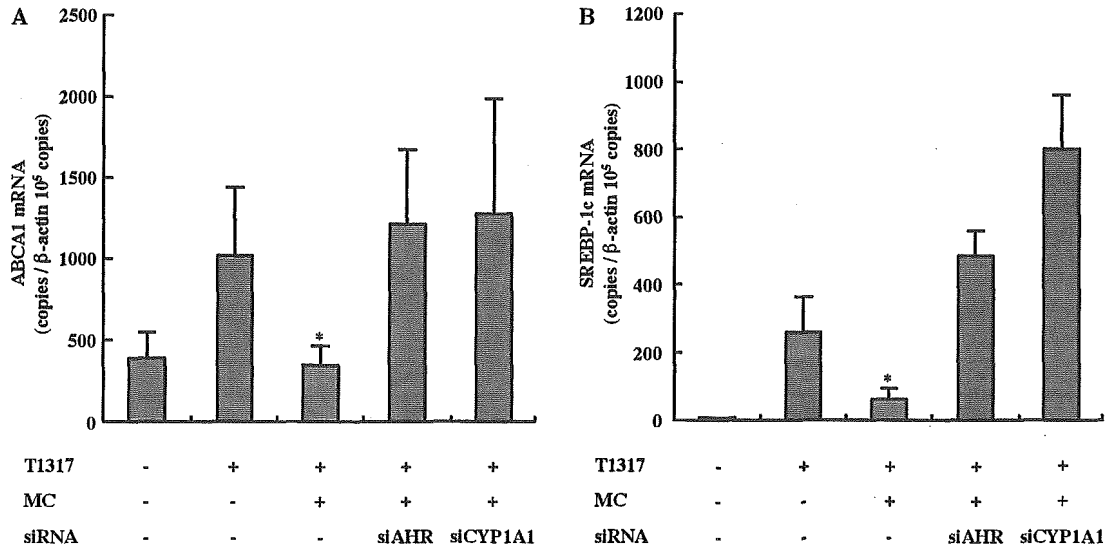

Fig. 4. E ects of siRNA for CYP1A1 on the MC-induced suppression of the expression of mRNAs for LXR-target genes. The expression of the genes regulated by LXR, ABCA1 (A) and SREBP-1c (B) was verified by real-time RT-PCR. HepG2 cells were transfected with pU6-siAHR, pU6-siCYP1A1 or pU6-control and cultured in the presence of 1 μM T1317 and 5 μM MC. After incubation for 24 h, total RNA was prepared from these cells and subjected to a real-time RT-PCR. Values in the figure represent the average ±SD from three independent experiments. *Statistically di erent ($p < 0.05$) relative to the cells treated with T1317 alone.

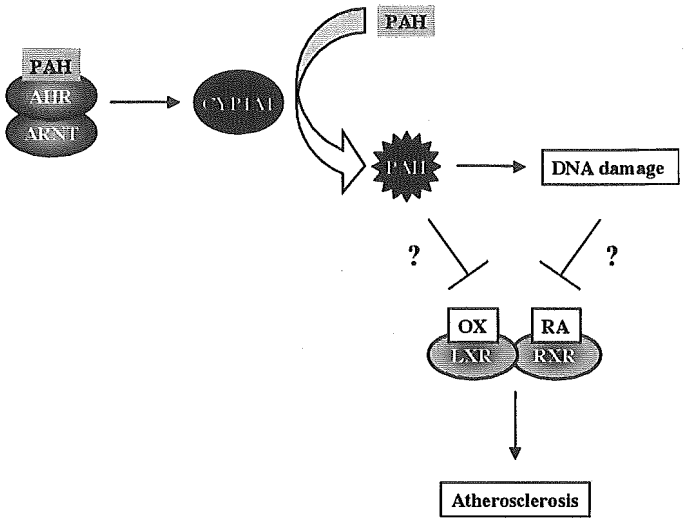

Fig. 5. Proposed mechanism(s) for the PAH-induced suppression of LXR-mediated signal transductions. PAH, polycyclic aromatic hydrocarbon; AHR, aryl hydrocarbon receptor; ARNT, AHR nuclear translocator; OX, oxysterols; RA, retinoic acid; LXR, liver X receptor; RXR, retinoid X receptor.

activity was restored (Fig. 3B). These results indicate that CYP1A1 induced by MC via an AHR-dependent mechanism plays direct roles in the MC-induced suppression of LXR-mediated transcriptional activity. In addition to the above results, we found that LXR-mediated transactivation was suppressed by MC when the pcDNA-hCYP1A1 was co-transfected into HepG2 cells with the pU6-siAHR (Fig. 3B), suggesting that CYP1A1, but not AHR, was a factor directly involved in the MC-induced suppression of LXR-mediated transcriptional activity.

To confirm that CYP1A1 is a critical factor for the MC-induced suppression of the expression of mRNAs for the LXR-target genes, we examined whether siCYP1A1 restored the MC-induced repression. The expression of mRNAs for ABCA1 and SREBP-1c, which are the LXR-targets, was induced by treatment of HepG2 cells with T1317 and was suppressed by co-treatment with MC (Figs. 4A and B). When the pU6-siAHR and pU6-siCYP1A1 were transfected into the cells, the expression levels of ABCA1 and SREBP-1c mRNAs were not suppressed by MC (Figs. 4A and B).

In the present study, we found that CYP1A1, but not AHR, played a key role in the suppression of LXR-mediated signal transductions by MC. It has been reported that the formation of the active metabolites of PAHs in White Carneau pigeons, which are susceptible to atherosclerosis, is greater than that in Show Racer pigeons, which are resistant to atherosclerosis [5]. Paigen et al. [6] reported that AKXL-38a mice, an AH-responsive strain, were more susceptible to MC-induced cancer and atherosclerosis than AKXL-38 mice, an AH-nonresponsive strain. Together with these results, it may be possible to hypothesize the mechanism of atherosclerosis induced by PAHs as follows (Fig. 5). First, PAHs bind to AHR and induce the expression of CYP1A1. Second, PAHs are metabolically activated by CYP1A1 induced by PAHs. Third, the LXR-originated signal transductions are suppressed by the active metabolites of PAHs directly or indirectly. Finally, the expression of the LXR-target genes is suppressed to cause atherosclerosis.

In conclusion, we propose in this paper that CYP1A1, but not AHR, is responsible for the MC-induced suppression of the expression of LXR-target genes, suggesting that the metabolic activation of PAHs by CYP1A1 is a process critical for atherosclerosis induced by PAHs.

Acknowledgments

This work was supported in part by a Grant-in-Aid from the Ministry of Education, Science, Sports and Culture of Japan, and from the Ministry of Health, Labor and Welfare of Japan.

References

[1] M.S. Zedeck, Polycyclic aromatic hydrocarbons: a review, J. Environ. Pathol. Toxicol. 3 (1980) 537–567.
[2] H.A. Hattemer-Frey, C.C. Travis, Benzo-a-pyrene: environmental partitioning and human exposure, Toxicol. Ind. Health 7 (1991) 141–157.
[3] S.S. Hecht, Tobacco smoke carcinogens and lung cancer, J. Natl. Cancer Inst. 91 (1999) 1194–1210.
[4] M.G. Knize, C.P. Salmon, P. Pais, J.S. Felton, Food heating and the formation of heterocyclic aromatic amine and polycyclic aromatic hydrocarbon mutagens/carcinogens, Adv. Exp. Med. Biol. 495 (1999) 179–193.
[5] M.W. Majesky, H.Y. Yang, E.P. Benditt, M.R. Juchau, Carcinogenesis and atherogenesis: di erences in monooxygenase inducibility and bioactivation of benzo[*a*]pyrene in aortic and hepatic tissues of atherosclerosis-susceptible versus resistant pigeons, Carcinogenesis 4 (1983) 647–652.
[6] B. Paigen, P.A. Holmes, A. Morrow, D. Mitchell, E ect of 3-methylcholanthrene on atherosclerosis in two congenic strains of mice with di erent susceptibilities to methylcholanthrene-induced tumors, Cancer Res. 46 (1986) 3321–3324.
[7] M.S. Denison, L.M. Vella, A.B. Okey, Structure and function of the Ah receptor for 2,3,7,8-tetrachlorodibenzo-*p*-dioxin. Species di erence in molecular properties of the receptors from mouse and rat hepatic cytosols, J. Biol. Chem. 261 (1986) 3987–3995.
[8] Y. Shimizu, Y. Nakatsuru, M. Ichinose, Y. Takahashi, H. Kume, J. Mimura, Y. Fujii-Kuriyama, T. Ishikawa, Benzo[*a*]pyrene carcinogenicity is lost in mice lacking the aryl hydrocarbon receptor, Proc. Natl. Acad. Sci. USA 97 (2000) 779–782.
[9] E.K. Silbergeld, T.A. Gasiewicz, Dioxins and the Ah receptor, Am. J. Ind. Med. 16 (1989) 455–474.
[10] O. Hankinson, The aryl hydrocarbon receptor complex, Annu. Rev. Pharmacol. Toxicol. 35 (1995) 307–340.
[11] F.P. Guengerich, Roles of cytochrome P-450 enzymes in chemical carcinogenesis and cancer chemotherapy, Cancer Res. 48 (1988) 2946–2954.
[12] A. Poland, J.C. Knutson, 2,3,7,8-Tetrachlorodibenzo-*p*-dioxin and related halogenated aromatic hydrocarbons: examination of the mechanism of toxicity, Annu. Rev. Pharmacol. Toxicol. 22 (1982) 517–554.
[13] S. Iwano, M. Nukaya, T. Saito, F. Asanuma, T. Kamataki, A possible mechanism for atherosclerosis induced by polycyclic

aromatic hydrocarbons, Biochem. Biophys. Res. Commun. 335 (2005) 220–226.
[14] N.S. Lee, T. Dohjima, G. Bauer, H. Li, M.J. Li, A. Ehsani, P. Salvaterra, J. Rossi, Expression of small interfering RNAs targeted against HIV-1 rev transcripts in human cells, Nat. Biotechnol. 5 (2002) 500–505.
[15] P.J. Paddison, A.A. Caudy, E. Bernstein, G.J. Hannon, D.S. Conklin, Short hairpin RNAs (shRNAs) induce sequence-specific silencing in mammalian cells, Genes Dev. 16 (2002) 948–958.
[16] C.P. Paul, P.D. Good, I. Winer, D.R. Engelke, E ective expression of small interfering RNA in human cells, Nat. Biotechnol. 5 (2002) 505–508.
[17] T.R. Brummelkamp, R. Bernards, R. Agami, A system for stable expression of short interfering RNAs in mammalian cells, Science 296 (2002) 550–553.
[18] G. Sui, C. Soohoo, B. A arel, F. Gay, Y. Shi, W.C. Forrester, Y. Shi, A DNA vector-based RNAi technology to suppress gene expression in mammalian cells, Proc. Natl. Acad. Sci. USA 99 (2002) 5515–5520.
[19] H.P. Ciolino, P.J. Daschner, G.C. Yeh, Resveratrol inhibits transcription of CYP1A1 in vitro by preventing activation of the aryl hydrocarbon receptor, Cancer Res. 58 (1998) 5707–5712.
[20] R.F. Casper, M. Quesne, I.M. Rogers, T. Shirota, A. Jolivet, E. Milgrom, J.F. Savouret, Resveratrol has antagonist activity on the aryl hydrocarbon receptor: implications for prevention of dioxin toxicity, Mol. Pharmacol. 56 (1999) 784–790.

Available online at www.sciencedirect.com
SCIENCE DIRECT®
Biochemical and Biophysical Research Communications 335 (2005) 220–226
BBRC
www.elsevier.com/locate/ybbrc

A possible mechanism for atherosclerosis induced by polycyclic aromatic hydrocarbons

Shunsuke Iwano, Manabu Nukaya, Tetsuya Saito, Fumie Asanuma, Tetsuya Kamataki *

Laboratory of Drug Metabolism, Graduate School of Pharmaceutical Sciences, Hokkaido University, Sapporo, Hokkaido, Japan

Received 14 July 2005
Available online 25 July 2005

Abstract

Polycyclic aromatic hydrocarbons (PAHs), aryl hydrocarbon receptor (AHR) ligands, induce atherogenesis. Liver X receptor (LXR) α is known to be involved in the control of cholesterol homeostasis. Thus, the purpose of this study was to investigate the e ects of 3-methlycholanthrene (MC), one of the PAHs, on LXRα-mediated signal transductions. We found that expression of mRNAs for ATP binding cassette A1, sterol regulatory element binding protein 1c (SREBP-1c), fatty acid synthase, and stearoyl-CoA desaturase was suppressed by treatment of HepG2 cells with MC. A luciferase reporter assay revealed that LXRα- and SREBP-1c-mediated transactivations were inhibited by MC via AHR. Based on these lines of evidence, we propose that down-regulation of the LXRα-regulated genes by PAHs is one of the causes responsible for atherosclerosis induced by PAHs.

Keywords: PAHs; LXR; ABCA1; SREBP-1c; FAS; SCD; Quantitative RT-PCR; Luciferase assay

Polycyclic aromatic hydrocarbons (PAHs)[1] are ubiquitous environmental contaminants that originate from multiple sources, including cigarette smoke, vehicle exhaust emissions, and industrial processes [1]. PAHs induce various toxicological e ects such as carcinogenesis, atherogenesis, and teratogenesis [2]. Several reports have suggested that cigarette-induced atherosclerosis is caused by PAHs [3–7]. PAHs are believed to show such toxicological e ects through the activation of AHR [8–10], which is identified as a ligand-activated transcription factor that controls the genes, including the *CYP1A1*, *CYP1A2*, and *CYP1B1* genes [11].

LXRα is a member of the nuclear hormone receptor superfamily and is activated by oxysterols [12,13]. It is abundantly expressed in organs including the liver, adipose, kidney, intestine, lung, adrenals, and macrophages [14]. LXRα acts as a cholesterol sensor to transactivate the genes that govern the transport, catabolism, and elimination of cholesterol [14]. ABCA1, a typical LXR target gene [15], transports phospholipids and cholesterol, and is known as a rate-limiting step in a reverse cholesterol transport [16]. Ligand-activated LXRα also up-regulates the *SREBP-1c* gene which belongs to the bHLH-Zip family of a transcription factor [17]. SREBP-1c enhances the transcription of the genes required for fatty acid synthesis and fatty acid elongation including FAS and SCD [18,19]. FAS and SCD produce oleoyl-CoA and palmitoeyl-CoA, which

* Corresponding author. Fax: +81 11 706 4978.
E-mail address: SNC78123@nifty.com (T. Kamataki).

[1] *Abbreviations:* ABC, ATP binding cassette; AHR, aryl hydrocarbon receptor; bHLH-Zip, basic helix-loop-helix-leucine zipper; CYP, cytochrome P450; DMEM, Dulbecco s modified Eagle s medium; FAS, fatty acid synthase; FBS, fetal bovine serum; LXR, liver X receptor; LXRE, LXR response element; MC, 3-methylcholanthrene; PAHs, polycyclic aromatic hydrocarbons; RT-PCR, reverse transcriptase-polymerase chain reaction; SCD, stearoyl-CoA desaturase; siRNA, short interference RNA; SRE, sterol regulatory element; SREBP-1c, sterol regulatory element binding protein 1c; T1317, TO-901317; TCDD, 2,3,7,8-tetrachlorodibenzo-*p*-dioxin.

0006-291X/$ - see front matter
doi:10.1016/j.bbrc.2005.07.062

are used for the esterification of cholesterol to detoxify the free cholesterol [20].

In the present study, we investigated the e ects of MC, which is one of the PAHs, on the LXRα-mediated signal transductions. We show herein that the activation of AHR by MC causes the down-regulation of the expression of mRNAs for ABCA1, SREBP-1c, FAS, and SCD, which are regulated by LXRα directly or indirectly. Possible mechanism(s) by which exposure to PAHs leads to atherosclerosis will also be discussed.

Materials and methods

Cell culture. Human hepatoma-derived HepG2 cells were purchased from RIKEN (Tsukuba, Japan). The HepG2 cells were maintained in DMEM (Nissui Pharmacy, Tokyo, Japan) supplemented with 10% FBS (Bio Whittaker, Warkersville, MD), non-essential amino acids (ICN, Aurora, OH), and 1 mM sodium pyruvate (Gibco-BRL, Rockville, MD) in 5% CO_2 at 37 C.

Plasmids. The 5′-flanking regions of the human *ABCA1* gene from 829 to +101, the human *SREEBP1c* gene from 1000 to 1, the human *FAS* gene from 927 to 1, and the human *SCD* gene from 1000 to 1 were obtained by PCR with respective sense primers, hABCA1-*Bgl*II-S (5′-GATCGATCAGATCTTAAGTTGGAGGTCTGGAGT GT-3′), hSREBP1c-*Bgl*II-S (5′-GAAGATCTGAACCCTAGAGCCT GTCACC-3′), hFAS-*Bgl*II-S (5′-GAAGATCTCGACTCCGCTCGC CACGTG-3′), and hSCD-*Bgl*II-S (5′-GAAGATCTTGACGGTTTCC ACAAAGAAG-3′), and antisense primers, hABCA1-*Hin*dIII-AS (5′-GATCGATCAAGCTTGCTCTGTTGGTGCGCGGA-3′), hSREBP 1c-*Hin*dIII-AS (5′-CCCAAGCTTGGCTCCGCGATCTGCGCC-3′), hFAS- *Hin*dIII-AS (5′-CCCAAGCTTTAGGCCGGCGCCGAC-3′), and hSCD-*Hin*dIII-AS (5′-CCCAAGCTTCGCGGTGCGTGGAG GTC-3′). The respective DNA fragments thus synthesized were digested with *Bgl*II and *Hin*dIII, and then inserted into the *Bgl*II and *Hin*dIII sites of a luciferase reporter plasmid, pGL3-basic vector (Promega, Madison, WI) to construct reporter plasmids, pABCA1-Luc, pSREBP-1c-Luc, pFAS-Luc, and pSCD-Luc. The p(LXRE)$_2$-TK-Luc was constructed by synthesizing oligonucleotides containing two copies of LXRE from mouse mammary tumor virus *LTR* gene promoter [21]. The p(SRE)$_2$-TK-Luc was constructed by synthesizing oligonucleotides containing two copies of SRE from mouse *SCD1* promoter [22]. The oligonucleotides were annealed and cloned into the *Xho*I site upstream of thymidine kinase promoter of pGL3-promoter vector (Promega). Full-length human LXRα cDNA was cloned into the *Bam*HI and *Eco*RI sites of pcDNA 3.1 mammalian expression vector (pcDNA-hLXRα) (Invitrogen, Carlsbad, CA). The pU6-siAHR as an siRNA expression plasmid for *AHR* gene silencing was constructed by using p *Silencer* 1.0-U6 siRNA Expression Vector (Ambion, Austin, TX). To construct hairpin siRNA expression cassette, two complementary oligonucleotides were synthesized, annealed, and ligated into the blunted *Apa*I site of the p *Silencer*. The sequences were 5′-GGTTTCAGCAGTCTGATGTCttca agagaGACATCAGACTGCTGAAACCCTTTTT-3′ and its complement, 5′-AGGGTTTCAGCAGTCTGATGTCtctcttgaaGACATCAG ACTGCTGAAACC-3′. This sequence cassette contained the oligonucleotides encoding 20-mer hairpin sequences specific to the human AHR mRNA at 438–458 position, a ttcaagaga loop sequence separating the two complementary domains, and a TTTTT terminator at the 3′-end [23–27].

Real-time RT-PCR analysis. Total RNA was prepared using GenElute Mammalian Total RNA Miniprep Kit (Sigma–Aldrich, St. Louis, MO). Reverse transcription reaction was performed by using First Strand cDNA Synthesis Kit for RT-PCR (AMV) (Roche Diagnostics, Indianapolis, IN). A quantitative real-time RT-PCR was carried out with a LightCycler using FastStart Reaction Mix SYBR Green I (Roche Diagnostics). The sequences of primer pair were designed as follows:

hABCA1: sense, 5′-TTTGTTCCTGTGTATTCTCTCA-3′; antisense, 5′-GGCAGCTTCTTGTCCTGGAG-3′,
hSREBP-1c: sense, 5′-CGGAGCCATGGATTGCACTTTC-3′; antisense, 5′-GATGCTCAGTGGCACTGACTCTTC-3′,
hFAS: sense, 5′-AACTCCAAGGACACAGTCACCAT-3′; antisense, 5′-CAGCTGCTCCACGAACTCAA-3′,
hSCD: sense, 5′-GGAAAGTGATCCCGGCATCGGAGA GCCAA-3′; antisense, 5′-GACAAAATAGTAGAATACCCCCC AAAGCC-3′, and
β-actin: sense, 5′-ATTGCTGACAGGATGCAGA-3′; antisense, 5′-AAGATCATTGCTCCTCCTGAGC-3′.

A reaction mixture contained 3 mM $MgCl_2$, 0.5 μM each primer, 1 FastStart DNA SYBR Green I mix, and 2 μL template cDNA in a final volume of 20 μL, and was collected into a LightCycler glass capillary. The details of thermal cycler program are as follows: Activation of the Taq DNA polymerase at 95 C for 10 min, 40 cycles of 95 C for 15 s, 68–70 C for 4–8 s, and 72 C for 20 s (transition rates of 20 C/s) and collection of the fluorescence values after each elongation step. The analysis of a melting curve was performed by annealing at 65 C for 15 s and redenaturation by raising the temperature to 95 C at a ramp rate of 0.1 C/s. To correct for di erences in both quality and quantity between samples, data were normalized using the ratio of the target cDNA concentration to that of β-actin.

Transient transfection and luciferase assay. The day before transfection, cells were plated at a density of 1 10^5 cells/well in a 12-well plate. Cells were transfected with 350 ng reporter plasmids (pABCA1-Luc, pSREBP-1c-Luc, pFAS-Luc, pSCD-Luc, p(LXRE)$_2$-TK-Luc or p(SRE)$_2$-TK-Luc), 100 ng pcDNA-hLXRα, and 50 ng pRL-TK vector (as an internal control for transfection) by using Fugene6 (Roche Diagnostics). The medium was changed to fresh DMEM containing MC (0.1 and 1 μM) (Sigma–Aldrich) and 1 μM T1317, a LXRα ligand (Sigma–Aldrich). Cells were harvested 36 h after starting the incubation. Luciferase activity was measured according to the method of the manufacturer. When siRNA expression vector was applied, cells were transfected with 300 ng pU6-siAHR or pU6-control, 100 ng pcDNA-hLXRα, 100 ng reporter plasmids (p(LXRE)$_2$-TK-Luc and p(SRE)$_2$-TK-Luc), and 50 ng pRL-TK vector. Twenty-four hours later, the medium was changed to DMEM containing MC (1 μM) and T1317 (1 μM). After 36 h of incubation, luciferase activity was measured.

Results and discussion

To examine whether or not the expression of genes regulated by LXRα was suppressed by PAHs, total RNA was prepared from HepG2 cells previously treated with 1 μM T1317 and 0.1, 1 or 10 μM MC. The expression of mRNAs for the genes regulated by LXRα was quantified by quantitative real-time RT-PCR method (Fig. 1). When HepG2 cells were treated with 1 μM T1317, the expression of mRNAs for the LXRα-target genes including ABCA1 and SREBP-1c was induced (Figs. 1A and B). The expression levels of ABCA1 and SREBP-1c mRNAs were increased by treatment with 1 μM T1317 and decreased by the co-treatment with

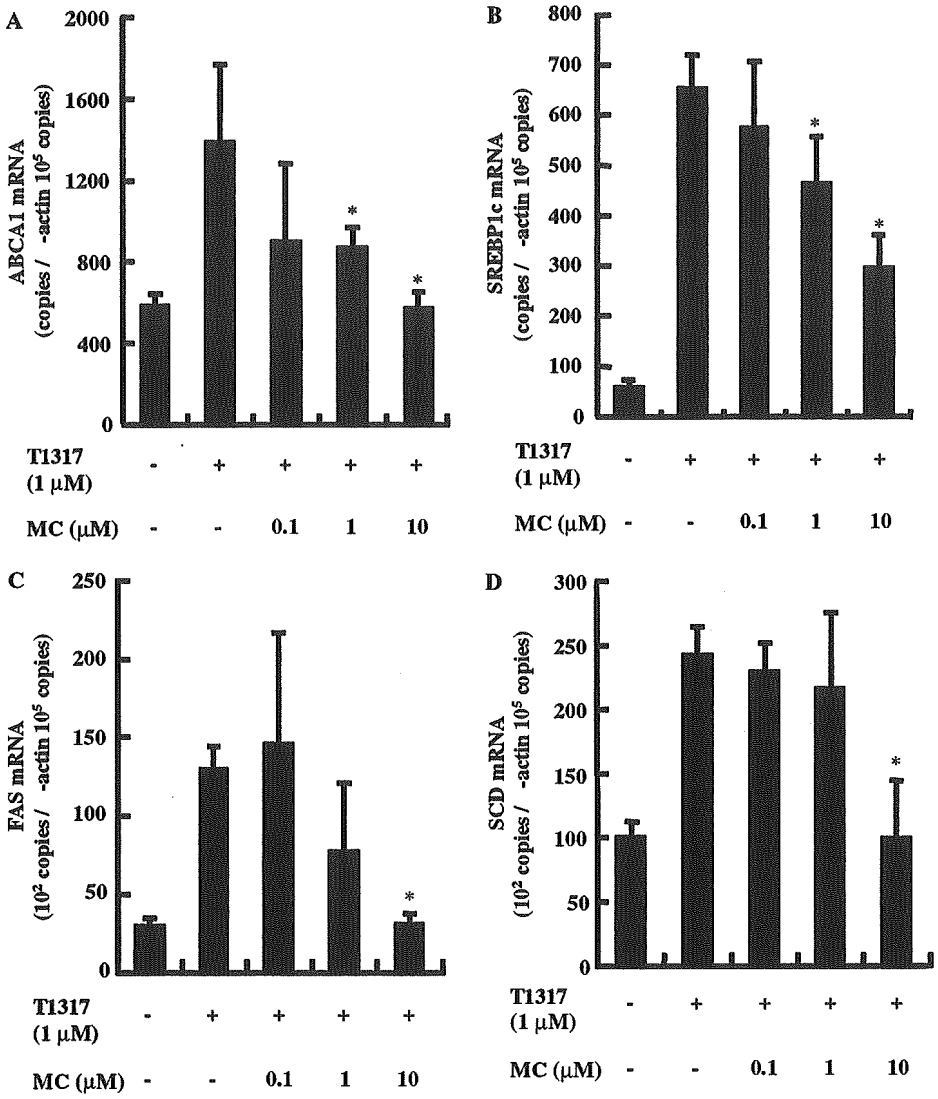

Fig. 1. Dose-dependent repression by MC of the expression of mRNAs for the genes regulated by LXRα. The expression of the genes regulated by LXRα, ABCA1 (A), SREBP-1c (B), FAS (C), and SCD (D) was verified by real-time RT-PCR. Total RNA (1 μg) prepared from HepG2 cells treated with 1 μM T1317, LXR ligand, and MC at various concentrations (0.1, 1, and 10 μM) was subjected to a real-time RT-PCR. The values represent the average ± SD from three independent experiments. *A statistically significant di erence ($p < 0.05$) relative to the cells treated with T1317 alone.

MC in a dose-dependent manner (Figs. 1A and B). The expression of mRNA for FAS, which is both the LXRα- and SREBP-1c-target genes [18], was also induced by T1317 in HepG2 cells and decreased by MC (Fig. 1C). In the case of SCD, which is the SREBP-1c-target gene [19], the mRNA expression was induced by T1317, and depressed by MC, dose-dependently (Fig. 1D). These results indicate that the expression of mRNAs for the LXRα-regulated genes induced by the activation of LXRα was suppressed by MC, suggesting that the LXRα-originated signals were repressed by PAHs.

To further support the possibility that the transcription of the genes regulated by LXRα was suppressed by PAHs, the e ects of MC on the transcriptional activity of LXRα- and SREBP-1c-target genes were examined by a luciferase reporter assay using a reporter plasmid including pABCA1-Luc, pSREBP-1c-Luc, pFAS-Luc, and pSCD-Luc (Fig. 2). When HepG2 cells were transfected with pcDNA-hLXRα in the presence of 1 μM T1317, the luciferase activity seen with pABCA1-Luc, pSREBP-1c-Luc, pFAS-Luc or pSCD-Luc was 3.8-, 3.6-, 4.7- or 3.4-fold higher than that seen in the absence of T1317, respectively (Figs. 2A–D). The luciferase activity seen with pABCA1-Luc, pSREBP-1c-Luc, pFAS-Luc or pSCD-Luc in the presence of 1 μM T1317 was decreased to a level of approximately 20–30% by 1 μM MC (Figs. 2A–D). Thus, it indicated that the transcription of essentially all of the LXRα and SREBP-1c target genes was suppressed by MC.

To further investigate the e ects of MC on the transcriptional activation through LXRα and SREBP-1c, a luciferase reporter assay was performed by using

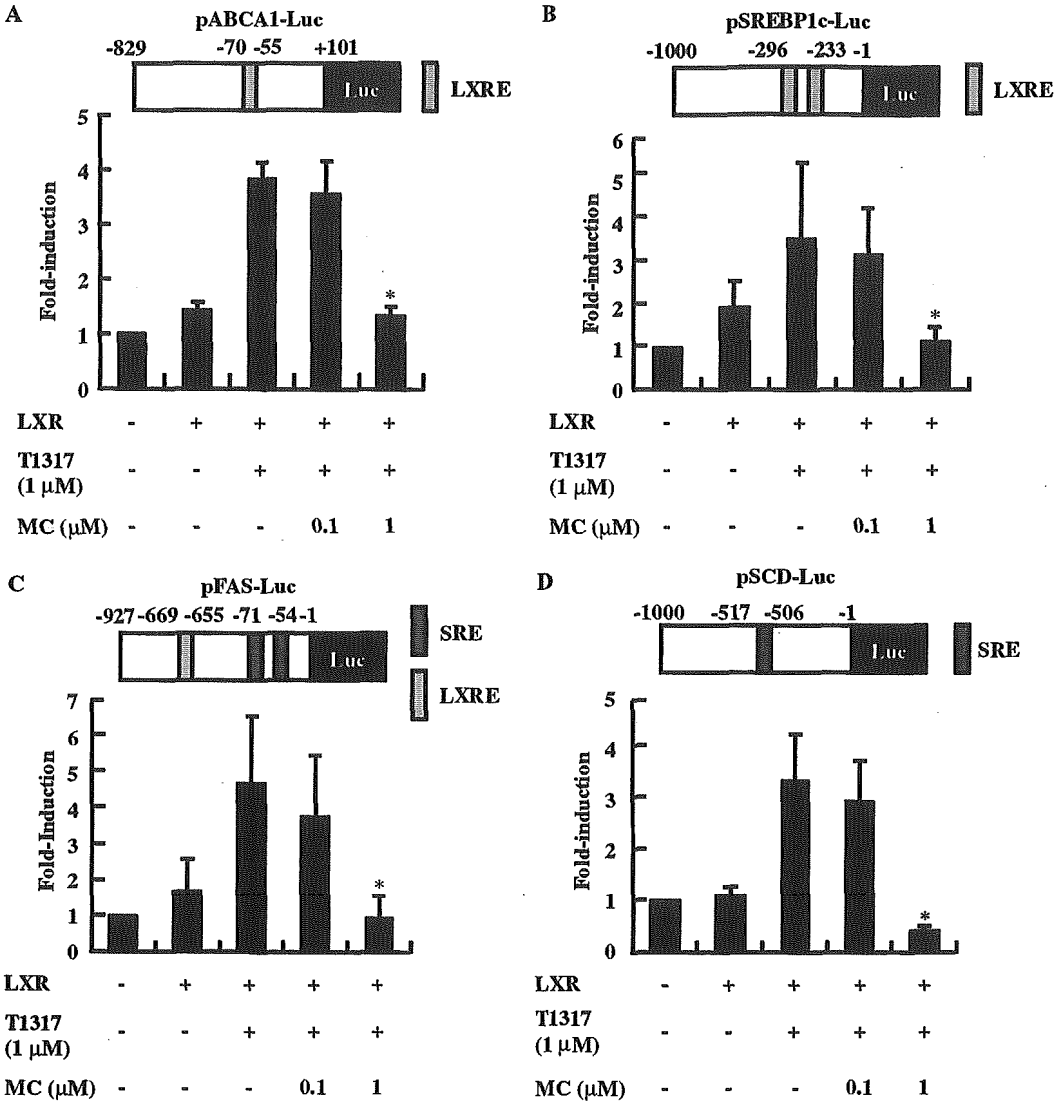

Fig. 2. Suppression by MC of the transcriptional activities of the genes regulated by LXRα. Luciferase reporter plasmids, pABCA1-Luc (A), pSREBP-1c-Luc (B), pFAS-Luc (C), and pSCD-Luc (D), were co-transfected into HepG2 cells with pcDNA-hLXRα. HepG2 cells were treated with T1317 (1 μM) and MC (0.1 and 1 μM). Luciferase activity was measured 36 h after incubation. The values represent the average ± SD from three independent experiments. *A statistically significant di erence ($p < 0.05$) relative to the cells treated with T1317 alone.

p(LXRE)$_2$-TK-Luc and p(SRE)$_2$-TK-Luc (Figs. 3A and B). When HepG2 cells were transfected with the p(LXRE)$_2$-TK-Luc or the p(SRE)$_2$-TK-Luc, and pcDNA-hLXR, the luciferase activity seen with the p(LXRE)$_2$-TK-Luc or the p(SRE)$_2$-TK-Luc was increased 55- or 2.2-fold by treatment with T1317, respectively (Figs. 3A and B). When HepG2 cells were treated with MC, the luciferase activities decreased to a level of 30–50% compared to that of control (Figs. 3A and B).

It has been reported that PAHs produce toxic e ects through the activation of AHR [8–10]. To confirm if AHR plays key roles in the repression of the transcriptional activation through LXRα and SREBP-1c by PAHs, we examined the e ects of siRNA expression plasmid to impair the expression of the *AHR* gene (Fig. 4). When HepG2 cells were transfected with pU6-siAHR, the protein level of AHR decreased (Fig. 4A), indicating that the siAHR could impair the effects of MC though AHR. Subsequently, we investigated whether the suppression of LXRα and SREBP-1c transactivation by MC was blocked by using the pU6-siAHR in HepG2 cells. The pU6-siAHR reversed the inhibition of LXRα and SREBP-1c transactivation by MC (Fig. 4B).

In the present study, we found that the transcriptional activity of the genes regulated by LXRα such as ABCA1, SREBP-1c, FAS, and SCD was down-regulated by MC depending on AHR. It has been reported that LXR regulates the ABC transporter genes including *ABCA1*, *ABCG5*, and *ABCG8*, which are responsible for cellular cholesterol e ux and dietary cholesterol absorption [14,28,29], and *CYP7A1* gene, which is

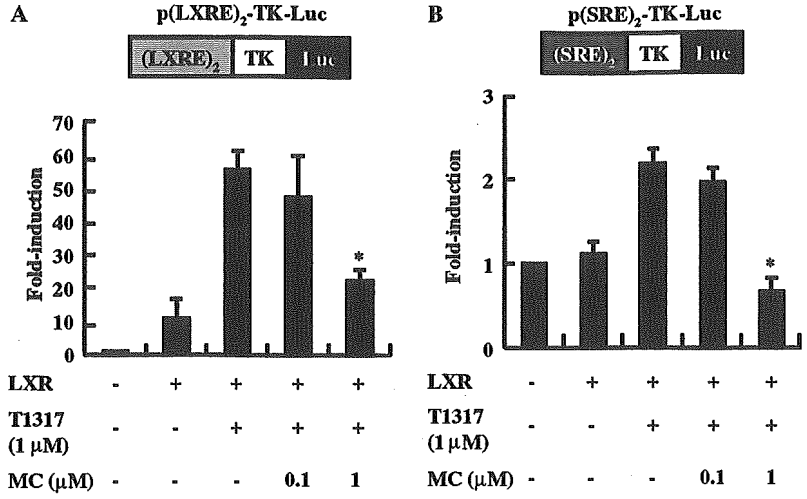

Fig. 3. Suppression by MC of transcriptional activities via LXRα and SREBP-1c. Luciferase reporter plasmids, $p(LXRE)_2$-TK-Luc (A) and $p(SRE)_2$-TK-Luc (B), were co-transfected into HepG2 cells with pcDNA-hLXRα. HepG2 cells were treated with T1317 (1 μM) and MC (0.1 and 1 μM). Luciferase activity was measured 36 h after incubation. The values represent the average ± SD from three independent experiments. *A statistically significant di erence ($p < 0.05$) relative to the cells treated with T1317 alone.

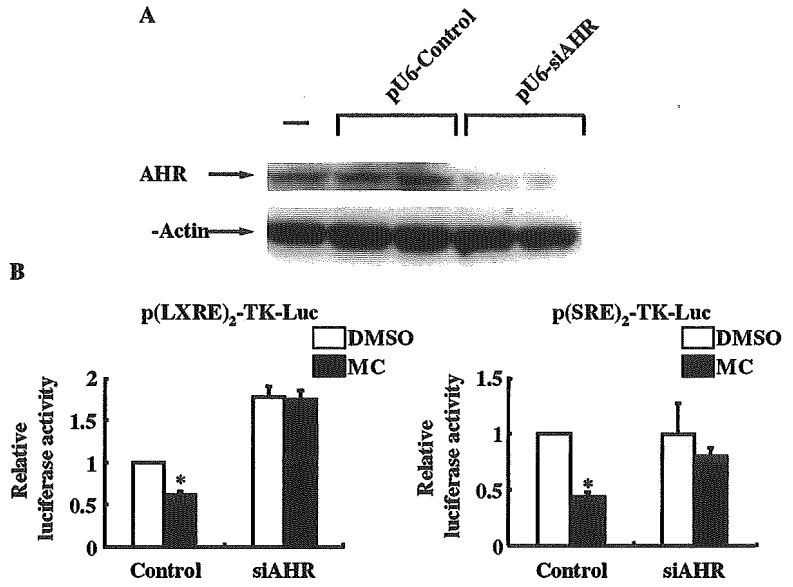

Fig. 4. E ects of siRNA for AHR on the down-regulation by MC of LXRα and SREBP-1c transactivation. (A) HepG2 cells were transfected with 300 ng pU6-control (control vector) or pU6-siAHR vector for AHR gene silencing. After 24 h, whole cell extracts (40 μg) were subjected to SDS–polyacrylamide gel electrophoresis and immunoblotting with AHR and β-actin antibodies. (B) HepG2 cells were co-transfected with pcDNA-hLXRα, pU6-siAHR, and $p(LXRE)_2$-TK-Luc or $p(SRE)_2$-TK-Luc. After 24 h incubation, the cells were treated with T1317 (1 μM) in the presence or absence of MC (1 μM). The luciferase activity was determined after 36 h of incubation. All transfection data represent means of at least three independent experiments. *A statistically significant di erence ($p < 0.05$) relative to the cells treated with T1317 alone.

involved in cholesterol catabolism [13]. Miyazaki et al. [20] reported that FAS and SCD were responsible for the esterification of cholesterol to produce oleoyl-CoA and palmitoyl-CoA, which is the detoxification pathway of free cholesterol. Thus, it is possible to assume that the atherosclerosis is induced by PAHs through the following mechanisms: (1) The exposure to PAHs causes the increase of free cholesterol level in plasma because of the suppression of LXR-target genes by PAHs via AHR (Fig. 5). (2) The detoxification of cholesterol is inhibited by PAHs via the down-regulation of the *FAS* and *SCD* genes, which are SREBP-1c-target genes, by PAHs through AHR (Fig. 5).

In conclusion, we demonstrated in this paper that the expression of the genes regulated by LXRα was suppressed by treatment with MC due to the disruption of LXRα-mediated transactivation via ligand-activated AHR. These molecular mechanisms probably account for the cause responsible for the atherosclerosis induced by PAHs.